Aus der Medizinischen Klinik und Poliklinik IV
der Ludwig-Maximilians-Universität München
Direktor: Prof. Dr. Martin Reincke

Investigation of protein stability as underlying molecular pathology in 21-hydroxylase deficiency

Dissertation

zum Erwerb des Doktorgrades der Medizin

an der Medizinischen Fakultät der
Ludwig-Maximilians-Universität zu München

vorgelegt von
Yiqing Chen
aus
Hefei, China
2019

Mit der Genehmigung der Medizinischen Fakultät
der Universität München

Berichterstatterin:	Prof. Dr. Nicole Reisch
Mitberichterstatterinnen:	Prof. Dr. Regina Fluhrer
	Prof. Dr. Beatrice Bachmeier
	Prof. Dr. Regina Ensenauer
Dekan:	Prof. Dr.med.dent. Reinhard Hickel
Tag der mündlichen Prüfung:	27.06.2019

To my parents, for their unconditional love, endless support and encouragement

Affidavit

Chen, Yiqing

I hereby declare, that the submitted thesis entitled

“Investigation of protein stability as underlying molecular pathology in 21-hydroxylase deficiency”

is my own work. I have only used the sources indicated and have not made unauthorised use of services of a third party. Where the work of others has been quoted or reproduced, the source is always given.

I further declare that the submitted thesis or parts thereof have not been presented as part of an examination degree to any other university.

Hefei, 27.06.2019 Chen, Yiqing

ABBREVIATIONS

17-OHP	17-hydroxyprogesterone
21-OHD	21-hydroxylase deficiency
3β-HSD	3β-hydroxysteroid dehydrogenase
4-PBA	4-Phenylbutyric acid
BSA	Bovine Serum Albumin
CAH	Congenital adrenal hyperplasia
COPII	Cytosolic coat protein II
CYP11B1	11β-hydroxylase
CYP11B2	Aldosterone synthase
CYP17A1	17α-hydroxylase
CYP21A2	21α-hydroxylase
DHEA	Dehydroepiandrosterone
DHT	Dihydrotestosterone
DOC	11-deoxycorticosterone
DTT	DL-Dithiothreitol
E2	Ubiquitin-conjugating enzymes
E3	Ubiquitin ligases
ER	Endoplasmic reticulum
ERAD	ER-associated degradation
ERQC	ER quality control
FBS	Fetal bovine serum
HLA	Human leukocyte antigen
hop	Hsp-organizing protein

HSP 70	Heat-shock protein70
LDL	Low-density lipoproteins
MHC	Major histocompatibility complex
NaCl	Sodium chloride
NC	Non-classic
P450scc	Side-chain cleavage cytochrome P450
PMSF	Phenylmethanesulfonylfluoride
PVDF	PolyvinylideneDifluoride
SDS	Sodium lauryl sulphate
SRD5A2	Steroid-5α reductase type 2s
StAR	Steroidogenic acute regulatory
SV	Simple-virilizing
SW	Salt-wasting
V2R	Vasopressin type-2 receptor

TABLE OF CONTENTS

1. Introduction

1.1 Background of 21-hydroxylase deficiency

Congenital adrenal hyperplasia (CAH) represents an autosomal recessive disorder characterized by a complex imbalance of adrenal steroids (Reisch, Arlt, & Krone, 2011). The deficiency of any adrenal enzyme required for glucocorticoid (GC) synthesis may lead to CAH. When glucocorticoid synthesis is impaired, ACTH is chronically elevated through the negative feedback system. This leads to overstimulation of the adrenal cortex and consequent hyperplasia of the adrenal gland and oversecretion of the steroid precursors. Depending on the location of the enzymatic block, there are many types of CAH including 11β-hydroxylase deficiency, 17α-hydroxylase deficiency, 21-hydroxylase deficiency (21-OHD), 3β-hydroxysteroid dehydrogenase deficiency, congenital lipoid adrenal hyperplasia, P450 oxidoreductase deficiency, etc. The most common form, 21-OHD due to mutations in the gene *CYP21A2*, is of particular interest since it accounts for more than 90% of all cases of CAH (Merke & Bornstein, 2005; Reisch et al., 2013). The mutations result in decreased glucocorticoid secretion with or without mineralocorticoid deficiency and excess androgens. Newborn screening programmes in most Western countries indicate that the incidence of the classical form of 21-OHD is one in 13,000 to 15,000 live births (Merke & Bornstein, 2005).

1.1.1 Biochemistry of steroid synthesis

The precursor of all steroid hormones is cholesterol. It is absorbed from the intestine and delivered to the adrenals by low-density lipoproteins (LDL) in the circulation (Figure 1). The rate-limiting step in steroidogenesis is the transport of cholesterol from cellular store to the inner mitochondrial membrane (Yaffe & Aranda, 2010). This transport is mainly governed by the steroidogenic acute regulatory (StAR) protein (Stocco & Clark, 1996). The first step of steroidogenesis is conversion of cholesterol to pregnenolone. This step is catalyzed by a mitochondral enzyme called side-chain cleavage cytochrome P450 (P450scc). Pregnenolone is transported back

into the cytosol and then enters the endoplasmic reticulum (ER) to feed the main steroid biosynthesis in the adrenal cortex including cortisol, aldosterone and dehydroepiandrosterone (DHEA).

The zona glomerulosa mainly contributes to the production of mineralocorticoids with the end product of aldosterone.

Glucocorticoids are mainly produced in zona fasciculata. In 21-OHD, the enzymatic block leads to accumulation of 17-hydroxyprogesterone (17-OHP) and a lack of cortisol.

In the zona glomerulosa, 17-hydroxyprenenolone is converted to DHEA by 17α-hydroxylase (CYP17A1) after conversion from pregnenolone (Rainey, Carr, Sasano, Suzuki, & Mason, 2002). The conversion from DHEA androstenedione is further catalyzed by 3β-HSD and then androstenedione can be transported in the circulation and metabolized to testosterone and dihydrotestosterone (DHT) in extra-adrenal tissue (W. L. Miller, 2009).

Mutations in *CYP21A2* can cause decreased production of aldosterone and cortisol combined with an excessive accumulation of precursors (Merke & Bornstein, 2005). At the same time, since androgen synthesis is not disrupted, precursors are shunted into the synthesis of adrenal androgens, which results in excessive production of adrenal androgens.

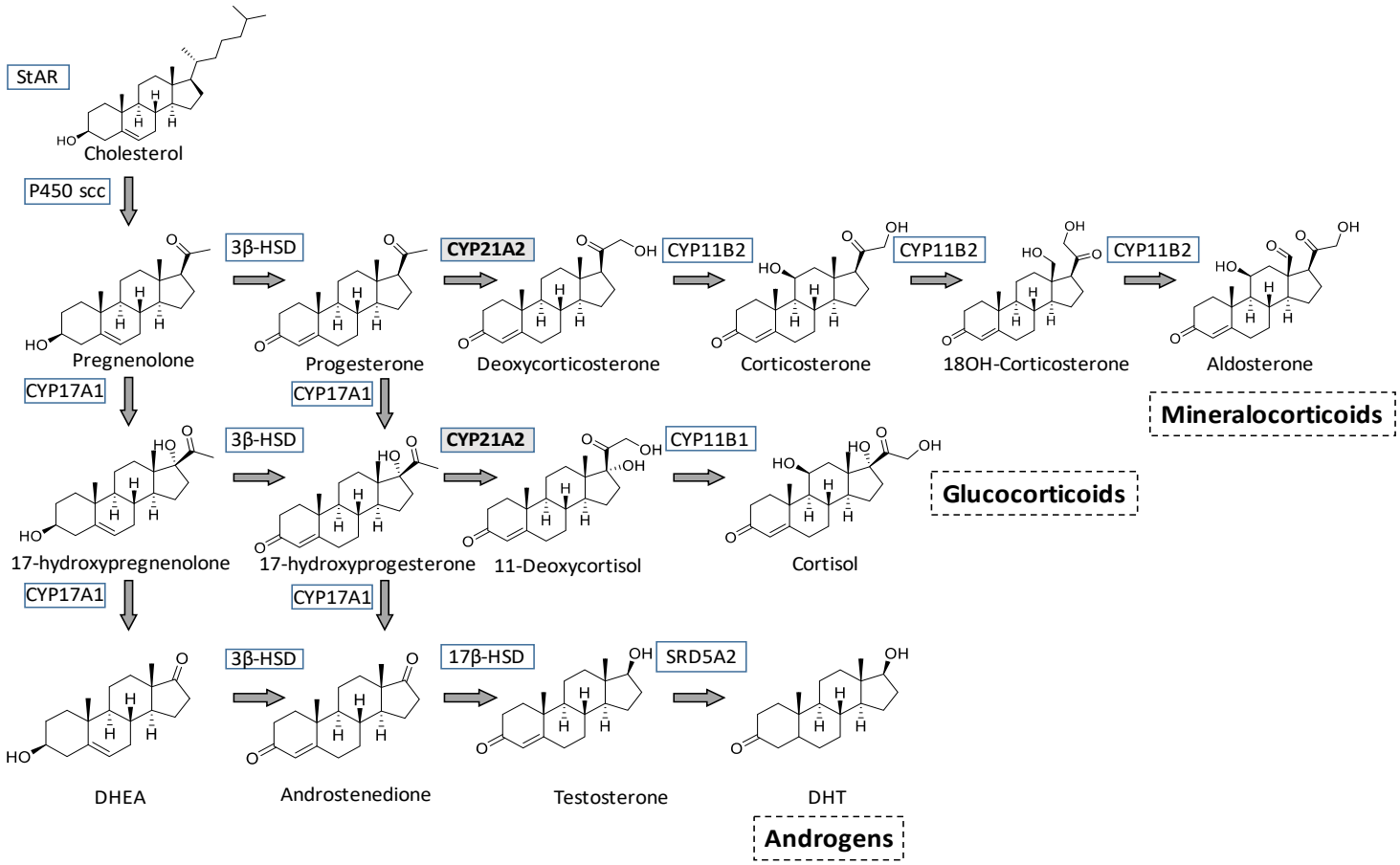

Figure 1 Steroid hormone biosynthesis*. The pathways for the synthesis of mineralocoticoids, glucocorticoids and androgens are arranged from left to right. The planar structures of the common precursor cholesterol and steroid hormone products are placed near the corresponding labels. Enzymes that catalyse each bioconversion are marked in boxes. StAR, steroidogenic acute regulatory protein; P450scc, side-chain cleavage cytochrome P450; 3β-HSD, 3β-hydroxysteroid dehydrogenase; CYP21A2, 21-hydroxylase; CYP11B2, aldosterone synthase; CYP17A1, 17α-hydroxylase; CYP11B1, 11β-hydroxylase; 17β-HSD, 17β-hydroxysteroid dehydrogenase; SRD5A2, steroid-5α reductase type 2; DHEA, dehydroepiandrosterone; DHT, dihydrotestosterone. The figure is adapted from Fig.1 from White & Speiser (White & Speiser, 2000).*

1.1.2 Molecular genetics of *CYP21A2*

Steroid 21-hydroxylase is encoded by a microsomal cytochrome P450 named *CYP21A2*. It is located in the human leukocyte antigen (HLA) major histocompatibility complex (MHC) locus on the short arm of chromosome 6 (6p21.3) with the homologous inactive pseudogene, *CYP21A1P* (*CYP21P*) (Anna Wedell, 2011). *CYP21A2* and the pseudogene are 3.3kb and have 10 exons with 98% homology of nucleotide sequences and 9 introns with 95% homology (Higashi, Yoshioka, Yamane, Gotoh, & Fujii-Kuriyama, 1986; White, New, & Dupont, 1986). They are close to and alternating with the genes encoding the fourth component of serum complement named factor *C4B* and *C4A* (Carroll, Campbell, & Porter, 1985; White et al., 1985). *C4/CYP21* with *RP* and tenascin X (*TNX)* comprises a genetic unit called RP-C4-CYP21-TNX (RCCX) module. The most common form of RCCX is bimodular (Figure 2) (Blanchong et al., 2000).

Due to the similarity and the proximity of *CYP21A2* and *CYP21A1P* and tandem repeats of RCCX region, misalignment may occur during meiosis followed by reciprocal recombination (also called unequal crossing over). Furthermore, small or large sequences may be transferred or inserted into genes or deleted during apparent gene conversion (Koppens, Hoogenboezem, & Degenhart, 2002). Approximately 65-70% gene conversions are point mutations (Z. Xu, Chen, Merke, & McDonnell, 2013). Around 95% of all mutations in *CYP21A2* causing 21-OHD occur because of the reasons stated above with remaining 5% of the mutations arising spontaneously without the involvement of the pseudogene in single families (A Wedell, Thilén, Ritzén, Stengler, & Luthman, 1994; White & Speiser, 2000).

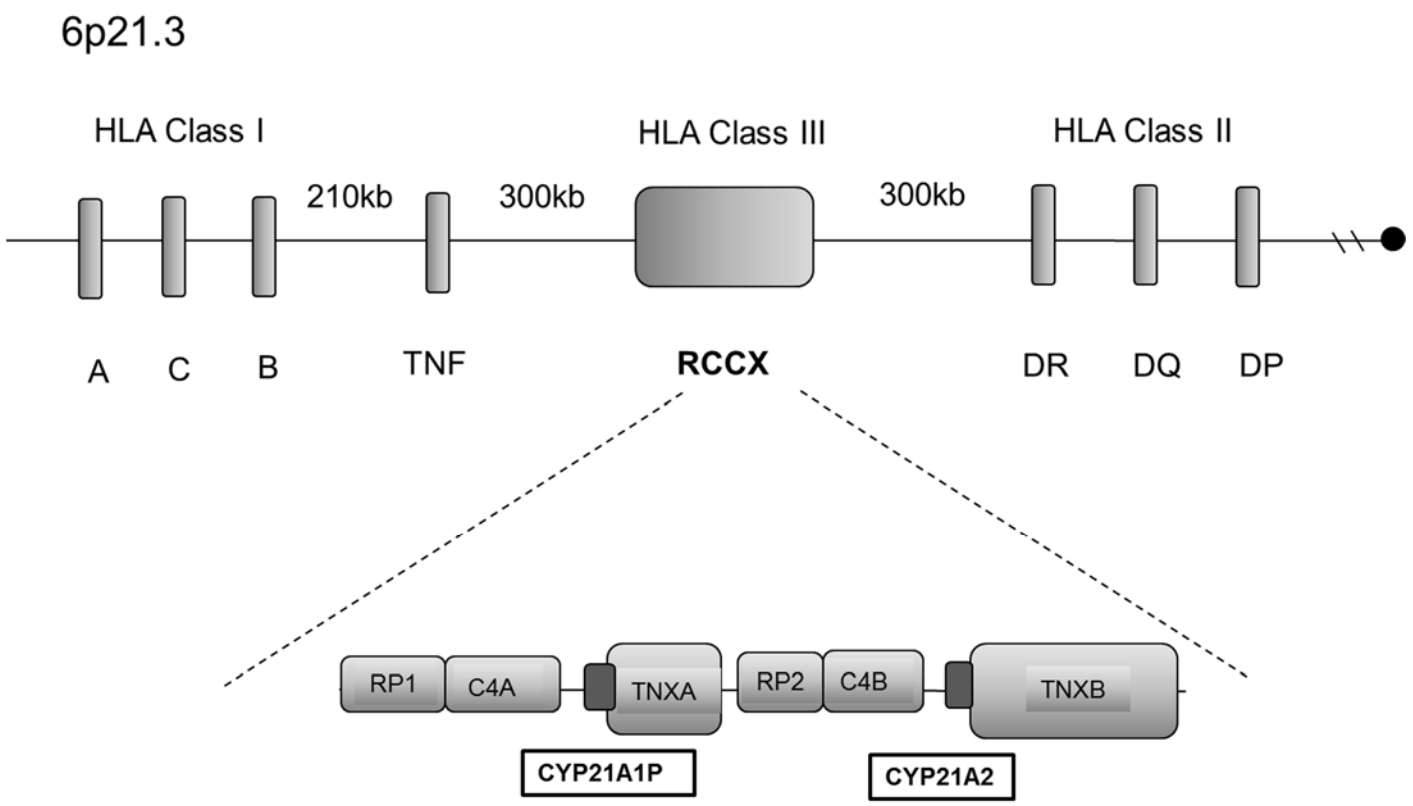

Figure 2 A schematic map of the HLA major histocompatibility complex on chromosome 6p21.3 containing a bimodular RCCX. *HLA-B is the nearest HLA Class I gene to CYP21A2, and HLA-DR is the nearest HLA Class II gene. The region in between is termed HLA Class III, where the RCCX module is located. Both the pseudogene and the functioning CYP21A2 gene are located in the RCCX module. HLA, human leukocyte antigen; RCCX, RP-C4-CYP21-TNX; TNF, tumor necrosis factor; TNXA, tenascin XA; TNXB, tenascin XB. The figure is adapted from Fig.11 from White & Speiser (White & Speiser, 2000).*

1.1.3 Clinical manifestations and treatment of 21-OHD

Decreased production of aldosterone and cortisol, combined with excessive production of androgens, leads to the clinical manifestations of 21-OHD. Due to the disease severity of 21-OHD, three phenotypes are recognized: salt-wasting (SW)21-OHD, simple virilizing (SV) 21-OHD and non-classic (NC)21-OHD. SW and SV are also known as classic 21-OHD.

Since lacking of 21-hydroxylase activity almost completely, SW 21-OHD is the most severe form of 21-OHD and accounts for 70% of classic 21-OHD (Pang, 2003). Newborns show a life-threatening salt loss together with prenatal virilization of external genitalia in affected females. On the contrary, SV 21-OHD patients do not have aldosterone deficits and are able to maintain electrolyte balance except during infections, trauma etc. Other symptoms like genital virilization in female newborns, accelerated growth and precocious puberty during early childhood are similar as the SW phenotype (Hargitai et al., 2001). The mildest form, NC 21-OHD is mainly diagnosed at a later age. Symptoms of hyperandrogenism like hirsutism, oligomenorrhea, acne and infertility show up during childhood and even adulthood. The majority of male NC 21-OHD patients are only diagnosed during family screening (Maria I New, 2006).

The aim of 21-OHD treatment is to prevent excessive production of androgens and adrenal crises by replacement of glucocorticoid and mineralocorticoid which are produced insufficiently. In addition, the targets also include optimising height, gonadal development and fertility.

Currently, steroid replacement is the main treatment, however, its side effects cannot be ignored. The long-term use of slightly supraphysiological glucocorticoid doses will bring metabolic and cardiovascular risks, such as obesity, hypertension, type 2 diabetes and dyslipidemia. Overtreatment with glucocorticoids and mineralocorticoids also suppresses growth, especially applying longer-acting glucocorticoids such as prednisone during puberty (Bonfig, Bechtold, Schmidt, Knorr, & Schwarz, 2007).

Thus, despite over 50 years' experience with steroid replacement therapy, the management of 21-OHD remains difficult and new therapeutic approaches with the least risk of side effects are needed.

1.2 Structural models of CYP21A2 protein

Previously, different homology models of human CYP21A2 protein structures based on other known P450 structures have been constructed (Mornet & Gibrat, 2000; Tiina Robins, Carlsson, Sunnerhagen, Wedell, & Persson, 2006). Many structure-based studies of the mutants causing 21-OHD have been performed using these models (Bleicken et al., 2009; Minutolo et al., 2011; Tardy et al., 2010). However, these models such as CYP2C5 and CYP51 proteins only have the sequence homology of 31% (Haider et al., 2013). Thus, the regions with low sequence homology could have high uncertainties. In addition, the substrate of the model based upon CYP51 protein structure was estriol, which led to a different ligand-binding site as that of CYP21A2. Overall, using the previous models of CYP21A2 protein would probably influence the accuracy of the molecular basis study of 21-OHD. In 2012, Zhao's group constructed a bovine CYP21A2 protein crystal structure complexed with 17OHP, and following them Haider's group extracted structural features from their template, aligned bovine and human sequences and derived a 3D structure of the humanized CYP21A2 protein (Haider et al., 2013; Zhao et al., 2012). Almost 79% sequence identity is shared between bovine and human enzyme and over 85% of known CYP21A2 protein variants are identical. Furthermore, almost all structural elements of human CYP21A2 protein can also be observed in bovine molecular models. Therefore, the model based on bovine showed the closed representation of human CYP21A2 protein structures. Recently, Pallan and co-workers expressed human CYP21A2 protein in E. coli and determined the human CYP21A2 protein crystal structure complexed with the substrate progesterone, which providing a better insight into structural and functional changes induced by 21-OHD -causing mutations (Pallan, Wang, et al., 2015).

In general, like other known P450 protein structures, the overall structure of the CYP21A2 protein contains 16 α-helices and 9 β-sheet domains (Figure 3). A

conserved hydrophobic P450 catalytic active site is well defined around a single heme prosthetic group. One 17-OHP/progesterone molecule is situated in the proximal portion of the substrate-binding site over the heme. The bovine CYP21A2 protein crystal structure showed that besides one 17-OHP binding in the active site, there was another 17-OHP located at the substrate entrance, waiting for the dissociation and moving into the active site (Haider et al., 2013; Zhao et al., 2012). Approximately 35% of the amino acid residues are in close proximity to the heme or substrate-binding sites. They are highly conserved and play an important role in maintaining the enzyme folding and activity. Therefore, it is easily to comprehend that protein variants occurring at these residues in the core of enzyme result often in SW21-OHD, the most severe 21-OHD phenotype. Conversely, according to the protein models of CYP21A2, SV and NC mutations are more typically positioned at peripheral regions or surface of protein. They may disrupt the transmembrane region, conserved hydrophobic patches or secondary bonds between residues. Therefore, in terms of active site of amino acid and the degree of mutation-induced damages in structural models of CYP21A2 protein, it could provide a comprehensive structural explanation for the severity of the 21-OHD.

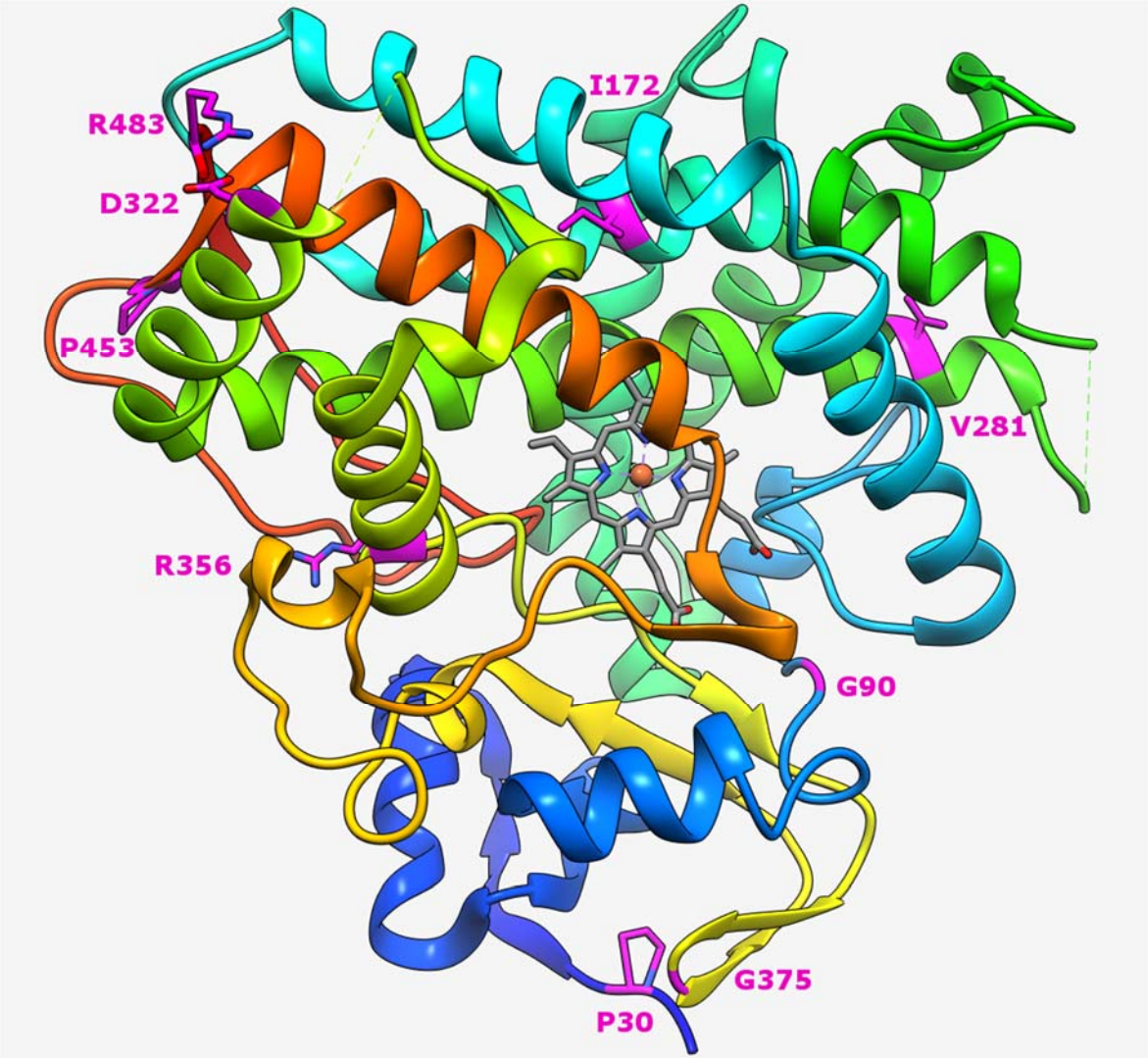

Figure 3 A humanized model of CYP21A2 protein. *The protein main chain is shown in ribbon mode and rainbow coloring, from N terminus (blue) to C terminus (red). Carbon, nitrogen, and oxygen atoms of the heme moiety are colored in grey, blue, and red, respectively, and Fe3+ is shown as an orange sphere. Secondary structure contains 16 α-helices and 9 β-sheets in rainbow coloring. Nine selected residues are colored in magenta.*

Increasing studies recently found that some amino acids residues have significant impact on the protein stability and folding in diseases such as hemochromatosis (de Almeida et al., 2007) and nephrogenic diabetes insipidus (Robben, Sze, Knoers, & Deen, 2006). As we have shown 9 residues in Figure 3 and Table 1, they form specific interactions with other residues from different helices or sheets, or provide right size fitting in limited space to maintain the secondary structure and conformational flexibility of protein. In this project, we will investigate 13 protein variants which are caused by point mutations from 9 residues as depicted in Figure 3. These 13 protein variants cover all three phenotypes of 21-OHD (salt-wasting, simple virilising, non-classic). All are based on naturally occurring, clinical relevant mutations with known and described clinical phenotypes well correlating with the residual enzyme activity *in vitro*. Since these residues are far from the heme and substrate binding site, they do not provide the direct disruption of heme and/or substrate binding, ensuring that active site is not directly affected. However, some studies found that these protein variants could induce the structural instability of CYP21A2 proteins (Haider et al., 2013; Zhao et al., 2012). Table 1 gives an overview of the selected residues with their known clinical phenotype, their localisation in the protein and the structural characteristic based on the bovine and human crystal structure of the protein. When the instable proteins emerging in the ER, they could be targeted by ER quality control (ERQC) system and finally degraded by ER-associated degradation (ERAD).

Table 1 Proposed structural basis of residues which that have been selected for investigation in this project.

Residues	***Localization***	***Mutations***	***Phenotype (residual enzyme activity in vitro progesterone)***	***Structural basis***
P30	N-terminal loop	P30L	NC (30%)(Tusie-Luna, Speiser, Dumic, New, & White, 1991)	It is lodged in a hydrophobic cavity constituted by L29, I59, V70, I374, Y377 and I379 on the surface of the protein, forms a hinge with P31 to help attach the P450 to the membrane.
		P30Q	SW (0%)(Lajic, Nikoshkov, Holst, & Wedell, 1999)	
G90	B-B' Loop	G90V	SW (0%)(Nunez, Lobato, White, & Meseguer, 1999)	It is adjacent to R91, which has a hydrogen bond with the propionate side chains of heme.
I172	E-Helix	I172N	SV (<2%)(Tusie-Luna, Traktman, & White, 1990)	The isoleucine residue is located in a hydrophobic pocket, surrounded by M186 and M187 on F-Helix.
V281	I-Helix	V281G	SV (3.9%)(Krone, Braun, Roscher, Knorr, & Schwarz, 2000)	V281 forms a hydrophobic patch together with some other hydrophobic residues on H-helix.
		V281L	NC (20%) (Tusie-Luna et al., 1990)	
D322	J-Helix	D322G	NC (27%)(Loidi et al., 2006)	There is a salt-bridge formation between R483 and D322.

Residues	***Localization***	***Mutations***	***Phenotype (residual enzyme activity in vitro progesterone)***	***Structural basis***
R356	K-Helix	R356Q R356W	SV (1.1%)(Lajic et al., 1997) SW (0%)(Chiou, Hu, & Chung, 1990)	R356 forms a hydrogen bonding with Q389 on K'-helix and Q462 on β8-β9 loop.
G375	β5 β6 loop	G375S	SW (<1%)(Lajic et al., 2002)	The β5 β6 loop, where G375 is positioned, can only suitable for the smallest amino acid residue.
P453	β8 Sheet	P453S	NC (20-46%)(Nikoshkov, Lajic, Holst, Wedell, & Luthman, 1997; Owerbach, Sherman, Ballard, & Azziz, 1992)	P453 is located in a hydrophobic pocket surrounded by L308 (helix I), L452 (β8-sheet), L458 (β8-β9 loop). A sharp turn begins from proline and introduces rigidity.
R483	C-terminal loop	R483Q R483W	NC (3.8%)(Stikkelbroeck et al., 2003) SW (0%)(Kharrat et al., 2004)	There is a salt-bridge formation between R483 and D322.

Source: Summary from the crystal structural model of human CYP21A2 protein and the humanized model of CYP21A2 protein based on bovine structure (Haider et al., 2013; Pallan, Lei, et al., 2015)

1.3 ER quality control (ERQC)

In eukaryotic cells, after nascent proteins are translated in the cytosol, they will be folded and assembled into mature proteins in specific compartments in the cells. Nearly one third human genome product is processed in the ER (Kelly & Balch, 2006).

As a central processor that controls protein folding and assembly, ER has developed a strict quality control system known as ERQC (Figure 4). ERQC is achieved through two execution pathways: (i) completely folded and assembled proteins can be exported from the ER to the Golgi complex (Lee, Miller, Goldberg, Orci, & Schekman, 2004). (ii) terminally unfolded or misfolded proteins are subjected to degradation by ERAD process (McCracken & Brodsky, 2005).

1.3.1 ERQC and ERAD of P450 proteins

CYP21A2 is a member of the cytochrome P450 family of enzymes. P450 proteins are all membrane bound and located in different subcellular compartments. Many of them including CYP21A2 protein reside in the membranes of ER. With assist of many chaperones and cellular proteins in the ER, proteins including P450 proteins can be folded correctly and avoided from targeting to the ERAD pathway (Lambert et al., 2001). It was found that heat-shock protein70 (HSP 70), HSP 90 and hsp-organizing protein (hop) bind to CYP2E1 and help it to stabilize. After the inhibition of HSP 90, increased degradation of CYP2E1 was found (Morishima et al., 2005).

When a P450 protein fails to acquire their native structure, it can be routed for the degradation progress known as ERAD (Correia & Liao, 2007). The most crucial step is marking P450 proteins by ubiquitylation. Chaperones and cochaperones can bind hydrophobic regions of misfolded proteins and help the misfolded proteins to be recognized by ubiquitin ligases (E3) (Park et al., 2007). E3 ligases can bridge the proteins with ubiquitin-conjugating enzymes (E2) (Zhen Xu et al., 2006). Then E3 ligases together with E2 transfer ubiquitin to the serine/threonine residues and less frequently lysine residues of targeted protein (Shimizu, Okuda-Shimizu, &

Hendershot, 2010). A cytoplasmic protein complex containing the AAA-ATPase cdc48p (also termed p97 in mammals) plays an important role in protein extraction from the membrane into cytosol (Acharya, Liao, Engel, & Correia, 2011; Chapman, Fry, & Kang, 2011). In cells containing mutated *cdc48*p gene, the degradation of CYP3A4 was shown to be inhibited (Liao, Faouzi, Karyakin, & Correia, 2006). Then the substrates can be transferred to the 26S proteasome for degradation by shuttle proteins which can bind to polyubiquitin chains of substrates and the proteasome subunits (J. Miller & Gordon, 2005).

1.3.2 The mechanism that protein-folding problems cause disease

ERQC is of great importance for maintaining proteins to function appropriately. However, when mutations cause misfolded and less functional forms of proteins and ERQC cannot control properly, as a result, many diseases could happen.

Firstly, improper ERAD can cause degradation or aggregation of proteins. ERAD is required for preventing the accumulation of misfolded or unfolded proteins. Thus, inefficient removal of misfolded proteins results in aggregation and subsequently influence the cell function. Similarly, overactive ERAD leading to elimination of variant proteins by degradation can also be the cause of development of some diseases. Since variant proteins still retain part of function even if they are misfolded, excessive elimination leads to loss-of-function. Furthermore, variant proteins that cannot achieve the correct folding encounters disturbed trafficking. Mutations in the N-terminal signal sequences lead to structural instability of the anchor of P450 proteins. Therefore, P450 proteins interactions with the ER membrane are disrupted, consequently causing enzyme function impairment (Soardi et al., 2008).

.

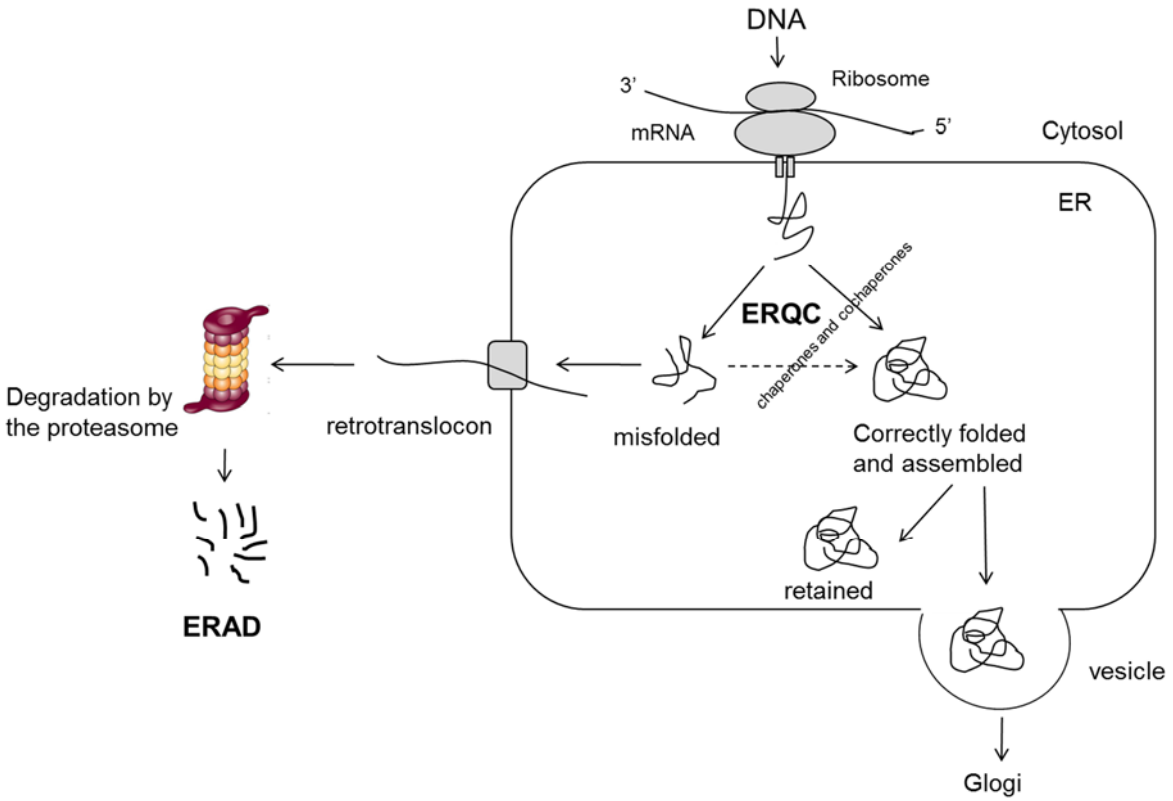

Figure 4 A simplified diagram of the processes involved in protein folding in the ER. *The polypeptides are translated from the ribosome directly into the ER, where they are folded and assembled into native functional proteins with the help of molecular chaperones and cochaperones. Then cytosolic coat protein II (COPII) coat mediates the most of proteins export from the ER to the Golgi complex via the secretory pathway, while a small fraction of proteins, including the* P450 proteins*, are retained in the ER. However, misfolding proteins are detected by ERQC and removed from the ER to cytosol through retrotranslocation. Finally, they are ubiquitinated and degraded by proteasomes as part of the ERAD system. The figure is adapted from Fig.1 from Ellgaard & Helenius (Ellgaard & Helenius, 2003).*

1.4 Therapeutic approaches in protein folding diseases

Numerous genetic diseases occur mainly due to protein misfolding. Treating these diseases is a great challenge. Some of the therapeutic approaches which have been found recently are described below.

1.4.1 Reduced temperature treatment

It has been proven that by reducing the incubation temperature for cell growth, the variant proteins can be treated. For example, low temperature at 27°C increased the ability of ΔF508CFTR to fold and the biochemical and functional expression at the cell surface (French et al., 1996; Heda & Marino, 2000). In addition to ΔF508CFTR, reduced temperature has been shown that the decreased degradation, the increased amount and stability of immature or mature proteins happened in different misfolded proteins such as vasopressin type-2 receptor (V2R) (Robben et al., 2006), AAT (Burrows, Willis, & Perlmutter, 2000), prion protein (Gu & Singh, 2004). The mechanism of reduced temperature treatment may be related with escaping the ER quality control system so that proteins can avoid degradation and process fully in the ER (Powell & Zeitlin, 2002). Moreover, under low temperature, protein increases its relative thermal stability to support themselves to export from ER (Aridor, 2007). Although reduced temperature cannot be achieved in mammal's body, these studies have provided a scientific approach that reduced temperature treatment can be manipulated in the cells.

1.4.2 Chemical chaperones

A number of studies published in recent years showed that a group of small molecular compounds can stabilize variant proteins without direct specific binding to the proteins. These compounds have been called 'chemical chaperones'. There are different classifications of them including osmolytes or hydrophobic compounds. The mechanisms involved are also diverse, including stabilization of misfolded proteins, raised production of proteins, decreased aggregation, change of the production or activity of endogenous chaperones, and intervention of nonproductive binding

interactions with other resident proteins (Perlmutter, 2002). Since the chemical chaperones do not bind with proteins specifically, they often have various pathologic conditions that they can apply for. Although most studies are conducted in cells, it is very theoretically attractive for protein folding diseases treatment.

4-Phenylbutyric acid (4-PBA) is a low-molecular weight fatty acid that has recently been found to be involved in protein folding with the chaperone activity. 4-PBA is known as a transcriptional regulator and inhibitor of histone deacetylase (Cuisset, Tichonicky, Jaffray, & Delpech, 1997; D'Anna, Tobey, & Gurley, 1980; Klehr, Schlake, Maass, & Bode, 1992). The oral form, Buphenyl® is an the U.S. Food and Drug Administration (FDA) approved new drug for the chronic management of some urea cycle disorders (Maestri, Brusilow, Clissold, & Bassett, 1996) and used in clinical trials for thalassemia (Collins et al., 1995) and sickle cell anemia (Resar et al., 2002). Ruvenstein et al. first studied the chaperone-like activity in IB3-1 cells and nasal polyp epithelial cells from cystic fibrosis (CF) patients (R C Rubenstein, Egan, & Zeitlin, 1997). They found that the molecular mass of CFTR increased and forskolin-activated chloride secretion restored. After that, the chaperone-like activity of 4-PBA is continually found in many other diseases including AAT deficiency (Burrows et al., 2000), nephrogenic diabetes insipidus (Robben et al., 2006) and hereditary hemochromatosis (de Almeida et al., 2007). Moreover, besides the cell model experiment, 4-PBA has been tested as a chemical chaperone in the mouse model by oral administration and well tolerated by the mice. The result showed an raised production of proteins in blood (Burrows et al., 2000). Since 4-PBA has been used safely in humans, it is a potential approach to protein folding diseases in the future.

1.5 Hypothesis

Through CYP21A2 protein molecular structures, impaired protein stability and the organization of secondary structures of protein can be the explanations for the severity of the 21-OHD clinical manifestations, indicating that 21-OHD may be in part a protein folding disease. Thus, in this research, we will investigate 13 protein variants

(Table 1) which are caused by point mutations and considered to be related with impaired protein stability. We hypothesize that 21-OHD derived from some specific mutations affects stability of CYP21A2 protein which can be enhanced through reduced temperature and chemical chaperone 4-PBAtreatment.

2. Aim of the thesis

1. To investigate protein half-life of naturally occurring, clinically relevant protein variants causing 21-OHD and to investigate the correlation between protein structure, functional data and clinical phenotype.
2. To evaluate CYP21A2 protein as a temperature-sensitive protein and reduced temperature treatment to enhance the half-life of CYP21A2 variant proteins *in vitro*.
3. To explore the possibility of using a chemical chaperone to enhance the half-life of CYP21A2 variant proteins *in vitro*.

3. Methods and materials

3.1 Site-directed mutagenesis and sequencing

Mutations were introduced into the pcDNA6/V5-His A, B and C mutagenesis vector containing pcDNA6/V5-His-*CYP21A2*, in which the full-length normal human *CYP21A2* cDNA had been cloned. Site-directed mutagenesis was performed using QuickChange site-directed mutagenesis kit. It allows site-specific mutation in virtually any double-stranded plasmid. Site-directed mutagenesis has already been performed in our lab by this method above and E. coli with mutated plasmid were ready to use for my work. Insertion of the mutations and the integrity of the insert were checked by direct sequencing.

3.2 Isolation of vector-DNA

Over-night transformed E. coli cultures were grown at 37 °C and 200 rpm in LB medium containing ampicillin 50 µg/mL. The next day, the cells were harvested by centrifugation at 6000 g for 15 minutes. DNA was extracted with PureYield Plasmid Midiprep System kit according to its manufacturer's protocol. The DNA UV absorbance was measured using a Nanodrop-ND1000.

3.3 Cell culture

In order to study the activity and half-life of *CYP21A2* protein variants, COS-7 cells were used for transient transfection. COS-7 cell line is derived from African green monkey kidney cells (CV-1) through transformation with a origin-defective Simian Vacuolating Virus 40 (SV40), which has integrated into COS cell chromosomal DNA (Aruffo, 2001). The main reason for using COS-7 cells is the high copy number achieved by the replication of the packaging plasmids in COS-7 cells (approximately 10,000 to 100,000 copies/cell within 48 hours post-transfection) (Aruffo, 2001).

COS-7 cell line was generated by YakovGluzman (Gluzman, 1981) and obtained from PD Dr. Soeren Gersting, Department of Department of Molecular Pediatrics, Dr. von Haunersches Kinderspital. COS-7 cells were cultured in RPMI 1640 medium supplemented with 10% fetal bovine serum and 1% penicillin / streptomycin. Cells were grown in sterile conditions in a humidified atmosphere (37°C and 5 % CO_2) in

cell culture flasks allowing adherent growth in a monolayer. Cells were passaged every second to third day with a seeding ratio of 1:6. Harvesting was achieved by trypsinization, and then cells were washed and resuspended in the medium. The numbers of passages for cell used in the experiments are between 10 to 20.

3.4 *In vitro* expression of *CYP21A2* protein variants, reduced temperature and 4-PBA treatment in COS-7 cells

Transfection of pcDNA6/V5-His-*CYP21A2*WT and mutant constructs was performed by using X-tremeGENE HP DNA Transfection Reagent. COS-7 cells were seeded in 48-well plates with approximately 75, 000 cells per well, and incubated for 24 hours at 37 °C. 0.1 μg DNA was transfected into cells transiently using 0.3μl of X-tremeGENE HP each well. In a subset of experiments cells were either (i) incubated at 30 °C for 48 hours or (ii) treated with 1mM 4-PBA at 37 °C for 24 hours. For the 4-PBA treatment, old culture medium was removed and cells were washed with DPBS after incubated with transfection reagents for 24h at 37°C. Then 500μl diluted 1mM 4-PBA in culture medium from 4-PBA stock solution was added to each well. Each subset has control groups treated at 37 °C for 48 hours and with blank medium respectively.

3.5 Protein isolation and concentration determination

Cells in 48-well plates were harvested for protein and washed twice with DPBS. Then cells were lysed by directly adding RIPA buffer supplemented with protease inhibitor cocktails on ice for 15 minutes and subsequently shaking at 300 rpm for 30min. Then the plates were centrifuged at 4000 rpm for 10 minutes at 4°C and supernatant from wells was collected to tubes. Protein concentration was measured using a protein assay based on the method of Bradford (Bradford, 1976). Bovine serum albumin (BSA) standards between 0 and 2 mg/ml were prepared in the same matrix as protein samples. Samples were measured on Multilabel Counter 1420 Victor and the protein concentrations were calculated by the reference values from the protein standard.

3.6 Limited proteolysis by proteinase K and western blot

Proteinase K is an endolytic protease that cleaves peptide bonds at the carboxylic sides of hydrophobic amino acid residues (aliphatic, aromatic and other hydrophobic amino acids). Stability of protein can be investigated by limited proteolysis with proteinase K. The proteolytic event is not dictated by the specificity of the protease K but the stereochemistry and flexibility of the protein substrate (Fontana et al., 2004; Gersting et al., 2008).

Wild type proteins (10 µg) and its variant proteins were digested with proteinase K (at a ratio of 1:20,000) at 37°C. Proteolysis was terminated at 0.5, 1, 2, 5, 10, 30, 60, and 120 min time points by addition of the 4 mM (final concentration) protease inhibitor phenylmethylsulphonyl fluoride (PMSF). Protein separation was achieved by running mixtures on a SDS-PAGE with 4–20 % gradient gels together with PageRuler pre-stained protein ladder. Electrophoresis was carried out for 45 minutes with 200 V in the Mini-PROTEAN II electrophoresis system filled with 1x running buffer. Size-separated protein on gels were then electroblotted to methanol activated Hybond-P polyvinylidenedifluoride (PVDF) membrane. The gels were placed in the 'transfer sandwich' (filter paper-gel-membrane-filter paper) in vertical buffer tank under 30 V for 60 minutes. The membranes were blocked in blotting-grade blocking solution for 1 hour and then incubated with a Mouse anti-V5 antibody overnight at 4°C. After TBST washing 3x 10 min with gentle shaking, membranes were incubated with HRP conjugated secondary antibodies for 1 hour. Detection was achieved by soaking the membranes using the SuperSignal West Femto Maximum Sensitivity Substrate kit according to the manufacturer's protocol. Chemiluminescence was monitored and the resulting protein bands were quantified by the ChemiDoc™ XRS+ System with Image Lab™ Software. Calculation of half-lives of degradation was measured by GraphPad Prism software version 6.0.

3.7 Materials

3.7.1 Laboratory equipment and software

Item	***Model***	***Manufacturer***
Analytics software	SPSS 19	IBM
Autoclave	VX-75	Systec
Benchtop centrifuge	5804R	Eppendorf
Benchtop centrifuge	5810R	Eppendorf
Biological safety cabinet	Safe 2020 Class II	Thermo
CO_2incubator	BBD 6220	Thermo
Diaphragm vacuum pump	MZ2C	Vacuubrand
Electrophoresis chamber	Mini-Protean 3	Bio-Rad
Electrophoresis chamber	Mini-Subcell GT	Bio-Rad
Electrophoresis chamber	Subcell GT	Bio-Rad
Electroporation device	PowerPac 200	Bio-Rad
Electroporation device	PowerPac™ HC	Bio-Rad
Gel imaging system	ChemiDoc™ XRS+ System	Bio-Rad
Graphing software	Graphpad prism 6	GraphPad
Hot plate magnetic stirrer	RCT basic	IKA
Image analysis software	Image Lab™ Software	Bio-Rad
Incubation cabinet	U30	Memmert
Microplate readers	Wallac 1420 Victor 2	Perkin Elmer
Microscope	TMS	Nikon
Microscope	Diaphot	Nikon
Mini Centrifuge	Galaxy mini C1213	VWR
Mixer	Vortex-Genie 2	IKA
PH-meter	SevenEasy™	Mettler-Toledo
Pipettes	Research® plus	Eppendorf

Item	*Model*	*Manufacturer*
Precision balance	770	KERN
Precision balance	440-45 N	KERN
Protein transfer device	Mini Trans-Blot Cell	Bio-Rad
Rolling mixer	RM5-35s 1732	Fröbel
Shaker	KS 125	IKA
Shaker incubator	G25	Eppendorf
Spectrophotometer NanoDrop	ND-1000	PeqLab
Thermal cycler	Primus 25 advanced	PeqLab
Thermal mixer	Thermomixer™	Eppendorf
Ultra-Low temperature freezer	HFU 586 Basic	Thermo
UV-transilluminator	GEL iX20	INTAS
Vacuum concentrator	5301	Eppendorf
Water bath	WB14	Memmert

3.7.2 Chemicals and consumables

Item	***Product Number***	***Company***
100 bp DNA Ladder	N3231S	New England Biolabs
4-PBA	BML-EI320-0001	Enzo
Agarose	35-1020	PeqLab
Blotting-grade blocker	1706404	BioRad
Bovine Serum Albumin (BSA)	5482	Sigma-Aldrich
Bromophenol blue	B0126	Sigma-Aldrich
Complete protease inhibitor cocktail	11836153001	Roche
ddH2O		Central Warehouse
Dichloromethane	106044	Merck-Millipore
DL-Dithiothreitol (DTT)	D0632	Sigma-Aldrich
DNA Loading Dye, 6x	R0611	Thermo
DPBS	14190	Gibco
Ethanol, absolute (EtOH)	108543	Merck-Millipore
Ethanol, technical (EtOH)		Central Warehouse
Ethylene diaminetetraacetic acid (EDTA)	E6758	Sigma-Aldrich
Fetal bovine serum (FBS)	10500064	Invitrogen
Glycerol	G5516	Sigma-Aldrich
Glycine	3908.2	Roth
H2O, sterile (Braun Aqua ad iniectabilia)		Central Warehouse
HRP substrate Western Lightning Plus-ECL	NEL103E001E	Perkin Elmer
LB-Agar	X969.1	Roth
LB-Medium	X968.1	Roth
Methanol	32213	Sigma-Aldrich
Mini-PROTEAN® TGX Stain-Free™ Precast Gels	456-8123	Bio-Rad
NADPH	N1630	Sigma-Aldrich
Nonidet P 40	74385	Fluka

Item	*Product Number*	*Company*
Page Ruler prestained protein ladder	26616	Thermo
Paraffin	107337	Merck-Millipore
Penicillin / streptomycin (Pen-Strep)	15140	Invitrogen
Phenylmethanesulfonylfluoride (PMSF)	P2721	DiaSorin
PVDF membrane	IPVH00010	Merck-Millipore
RNase-free water	129112	Qiagen
RotiQuant	0118.2	Roth
RPMI 1640	61870	Gibco
Sodium chloride (NaCl)	1064040500	Merck-Millipore
Sodium lauryl sulfate(SDS)	L3771	Sigma-Aldrich
Tris base	T6606	Sigma-Aldrich
Tween 20	P1379	Sigma-Aldrich

3.7.3 Buffers and solutions

3.7.3.1 Buffer

RIPA Buffer

Component	*Final concentration*
EDTA pH 8 [0.5 M]	1 mM
NaCl [2.5 M]	150 mM
NP-40	1%
Tris pH7.4 [1M]	50mM

The buffter was stored at 4°C.

5x Running Buffer

Component	*Final concentration*
Glycine	1 M
SDS [10%]	0.5 %
TrisBase	125 mM

Transfer Buffer

Component	*Final concentration*
Glycine	0.2 M
Methanol	20 %
TrisBase	25 mM

4x TBS (pH 7.6)

Component	*Final concentration*
NaCl	0.5 M
TrisBase	80 mM

The buffer was adjusted the pH to 7.6 using 1 M HCl and kept at 4°C.

1 x TBS (pH 7.6)

Component	*Final concentration*
NaCl	0.5 M
TrisBase	80 mM
Tween	0.1 %

The buffer was adjusted the pH to 7.6 using 1 M HCl and kept at 4 °C.

SDS sample buffer (6x)

Component	**Final concentration**
Bromophenol blue	0.06 %
DTT	0.6 M
Glycerol	30%
SDS	12 %
Tris pH6.8 [0.5M]	0.06 M

The solution was stored as aliquots at -20 °C.

3.7.3.2 Solution

Solution	***Concentration***
1st antibody solution	1:6,667 in blotting-grade blocking solution
2nd antibody solution	1:10,000 in blotting-grade blocking solution
4-PBA stock solution	100 mM in nuclease-free water with filtration
Ampicillin stock solution	100 mg/ml in nuclease-free water with filtration
Blotting-grade blocking solution	10 % in 1x TTBS
BSA solution	10 mg/ml in proteinase inhibitor solution
LB medium	25 g/l in ddH_2O
PMSF solution	4 mM in absolute ethanol
Proteinase inhibitor solution	one tablet for 10 ml RIPA buffer
Proteinase K solution	1:20000 in RIPA buffer

3.7.4 Kit

Item	***Product***	***Company***
PureYield™ Plasmid Midiprep System	A2495	Promega
PureYield™ Plasmid Miniprep System	A1222	Promega
QuickChange site directed mutagenesis kit	200518	Agilent Technologies

3.8 Statistical analyses

Values are expressed as mean ± standard error of mean (SEM). Unpaired two-sample Student t-test was used for analysis of significance, with p values of $p<0.05$ and below considered significant.

4. Results

Through limited proteolysis by proteinase K experiment, we finally calculated half-lives of WT and all variant proteins. Compared with WT, all variant proteins showed reduced half-lives ($p < 0.05$ or < 0.01), indicating that CYP21A2 variant enzymes were more susceptible to degradation by protease K (Figure 5, Table 2). Substantially reduced half-lives were detected in the variant proteins P30Q, G90V, R356W and R483W, which had half-lives less than 1min.

We then determined mean half-lives of WT and variant proteins after cells had been cultivated at 37°C and 30°C (Figure 5). A student's T-test showed there was no difference in half-lives of WT, I172N, V281G, V281L, D322G, G375S and P453S at the different temperatures ($p>0.05$). Other variant proteins (P30L, P30Q, G90V, R356Q, R356W, R483Q and R483W) showed significantly longer half-lives ($p < 0.05$ or < 0.01) at 30°C degree. This result suggested that reduced temperature could stabilize some but not all variant proteins and prevent them from rapid degradation.

We then examined whether the chemical chaperone 4-PBA influences the half-lives of CYP21A2 variant proteins (Figure 6, Table 2). For these experiments, we chose WT and variant proteins which had a prolonged half-life after cells had been cultivated at 30 °C. If these proteins can be also stabilized by reduced temperature and 4-PBA, it will illustrate that the rescue was specific for a limited set of variant proteins. Furthermore, we also selected I172N for further investigations although we did not observe an effect of temperature here as this is a clinically highly relevant protein variant and as others have shown altered conformation of the I172N mutant protein by increasing concentrations of proteinase K digestion previously (Hsu et al., 1996). As shown in the histogram half-lives of all variant proteins except I172N were prolonged by 4-PBA ($p < 0.05$ or < 0.01), and interestingly two (R356Q and R483W) of them even had longer half-lives than WT, indicating that 4-PBA can markedly enhance the half-life of some variant proteins. WT and I172N did not show any augment on half-lives ($p>0.05$), which fits to our previous observation that I172N did not show any change in half-life based on different temperature. In summary, 4-PBA treatment

induced a significant effect on stabilization of some CYP21A2 variant proteins. The respective Western Blot results are summarized in Figure 7. These figures show representative Western Blot results and the calculated protein decay curves resulting from the proteinase K experiments described above. All calculated half-lives are given also in Table 2. Overall, reduced half-life caused by CYP21A2 protein variants could be reversed by reduced temperature and 4-PBA treatment.

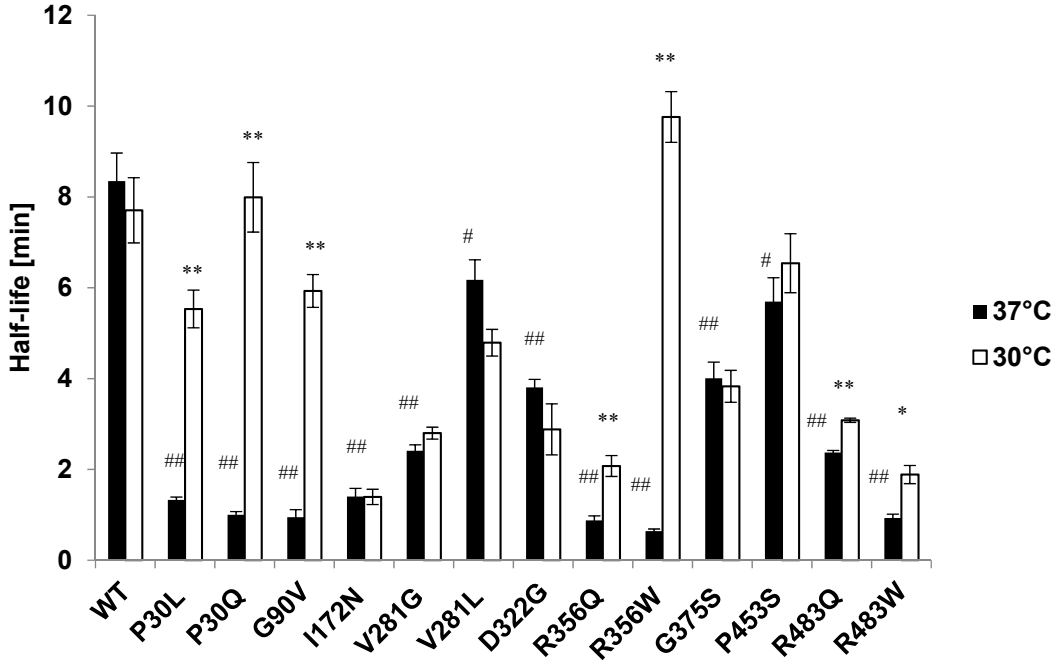

Figure 5 Half-lives of WT and variant proteins at 37°C and 30°C in minutes. *Degradation of the WT and variant proteins were probed by western-blotting analyses. Densitometric analysis was performed using Imagequant software. Half-life was calculated using a one-phase exponential decay model and given in mean ± SEM of n= at least 3 independent experiments. Black bar represented half-life at 37°C, while grey bar indicated half-life at 30°C.* $^{\#}$ *- p<0.05,* $^{\#\#}$ *- p<0.01 denote significant differences of the half-lives of variant proteins at 37°C compared with the half-life of WT at 37°C.* - p<0.05, ** - p<0.01 denote significant differences of the half-life at 30°C compared with the corresponding half-life at 37°C.*

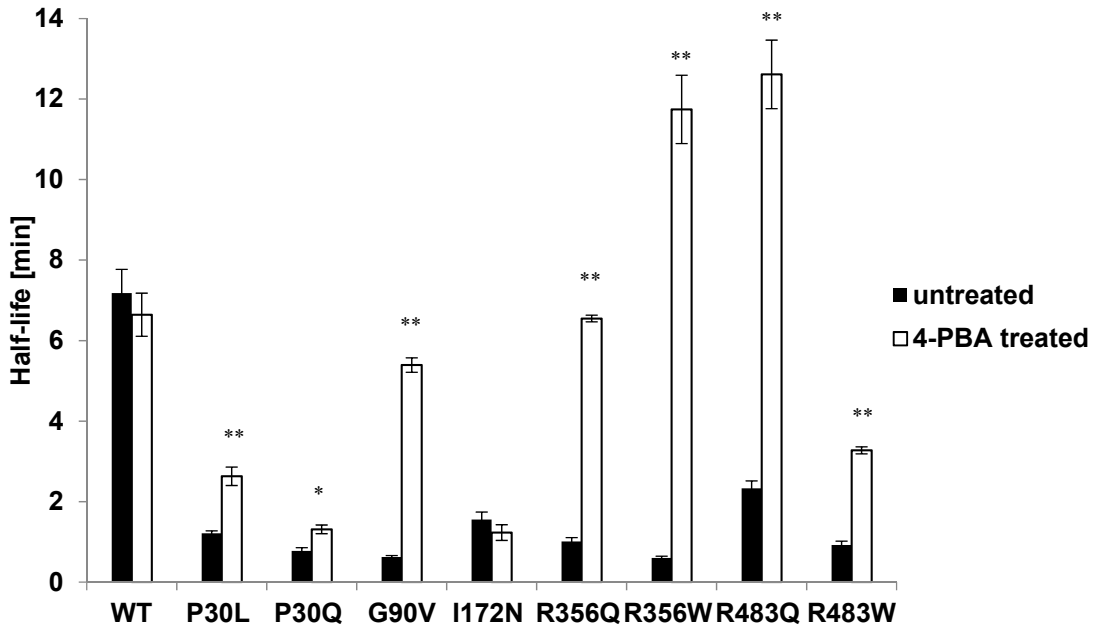

Figure 6 Half-lives of WT and variant proteins with and without 4-PBA treatment. *Each value represents mean ± SD of three independent experiments performed. Black bars represent half-life without 4-PBA treatment, while white bars indicate half-life with 1 mM 4-PBA treatment. * - p<0.05, ** - p<0.01 denote significant differences compared with the corresponding no treatment group. ## - p<0.01 denotes significant differences compared with the WT group.*

A

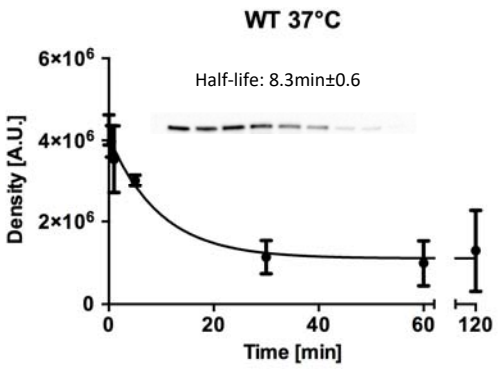
WT 37°C
Half-life: 8.3min±0.6
Density [A.U.]
Time [min]

B

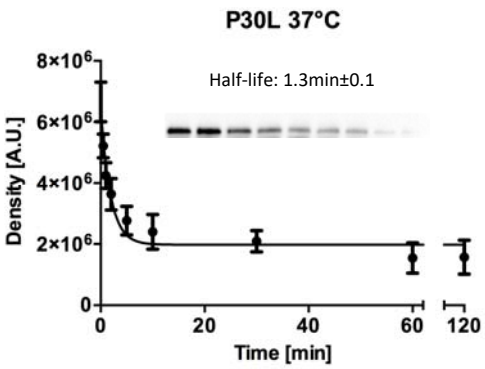
P30L 37°C
Half-life: 1.3min±0.1
Density [A.U.]
Time [min]

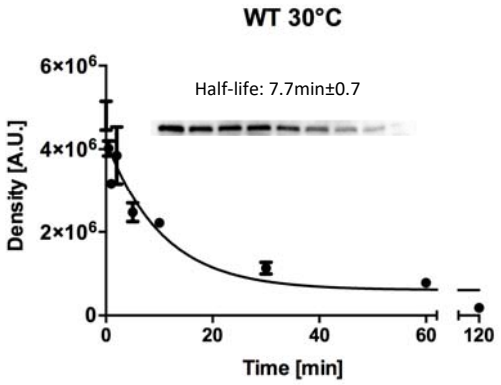
WT 30°C
Half-life: 7.7min±0.7
Density [A.U.]
Time [min]

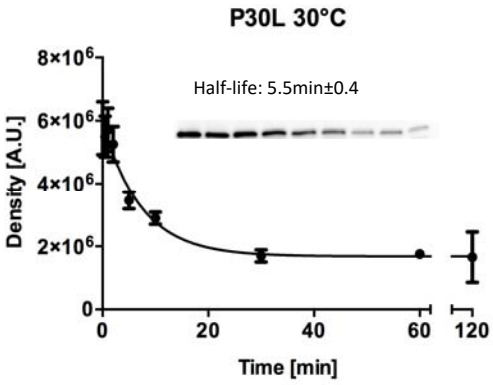
P30L 30°C
Half-life: 5.5min±0.4
Density [A.U.]
Time [min]

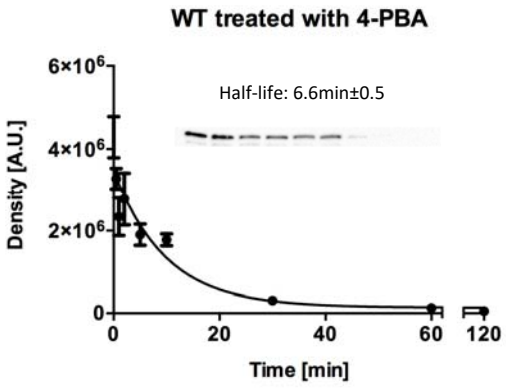
WT treated with 4-PBA
Half-life: 6.6min±0.5
Density [A.U.]
Time [min]

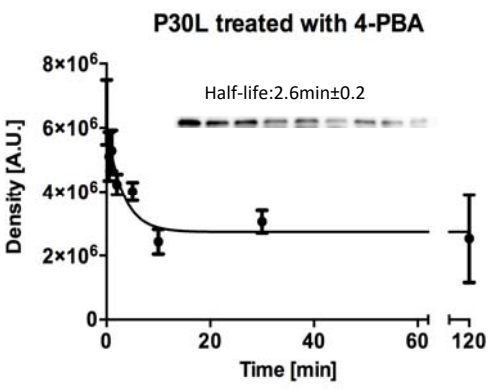
P30L treated with 4-PBA
Half-life:2.6min±0.2
Density [A.U.]
Time [min]

C

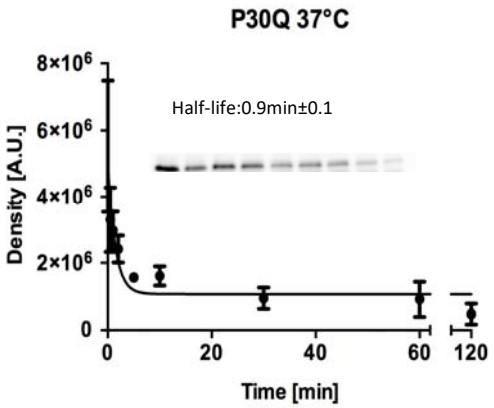
P30Q 37°C
Half-life:0.9min±0.1
Density [A.U.]
8×10^6
6×10^6
4×10^6
2×10^6
0
0
20
40
60
120
Time [min]

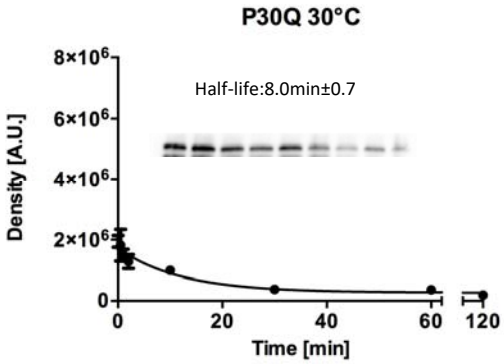
P30Q 30°C
Half-life:8.0min±0.7
Density [A.U.]
8×10^6
6×10^6
4×10^6
2×10^6
0
0
20
40
60
120
Time [min]

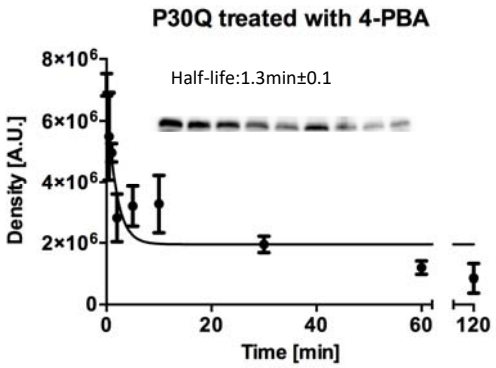
P30Q treated with 4-PBA
Half-life:1.3min±0.1
Density [A.U.]
8×10^6
6×10^6
4×10^6
2×10^6
0
0
20
40
60
120
Time [min]

D

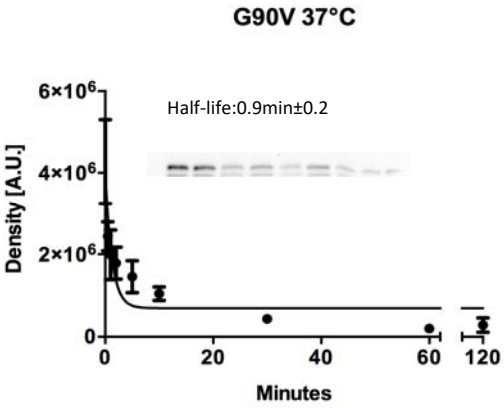
G90V 37°C
Half-life:0.9min±0.2
Density [A.U.]
6×10^6
4×10^6
2×10^6
0
0
20
40
60
120
Minutes

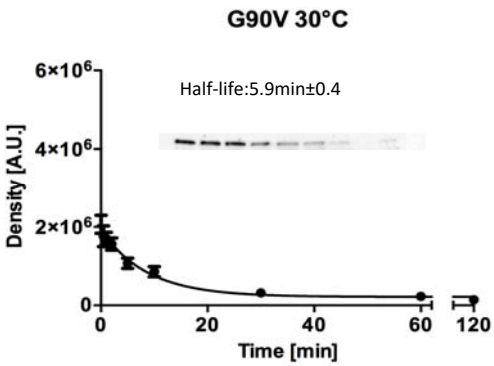
G90V 30°C
Half-life:5.9min±0.4
Density [A.U.]
6×10^6
4×10^6
2×10^6
0
0
20
40
60
120
Time [min]

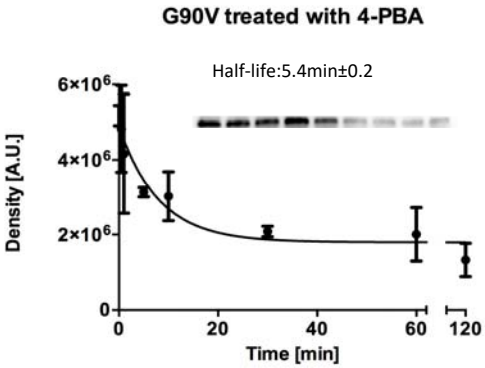
G90V treated with 4-PBA
Half-life:5.4min±0.2
Density [A.U.]
6×10^6
4×10^6
2×10^6
0
0
20
40
60
120
Time [min]

E

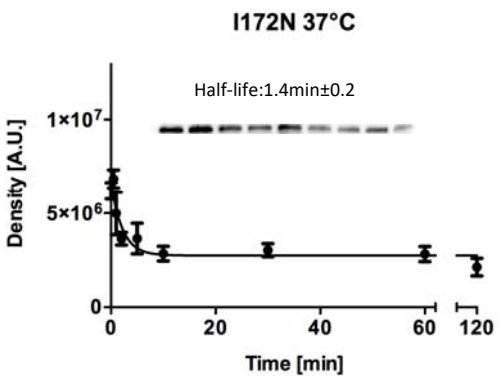
I172N 37°C
Half-life:1.4min±0.2
Density [A.U.]
1×10^7
5×10^6
0
0
20
40
60
120
Time [min]

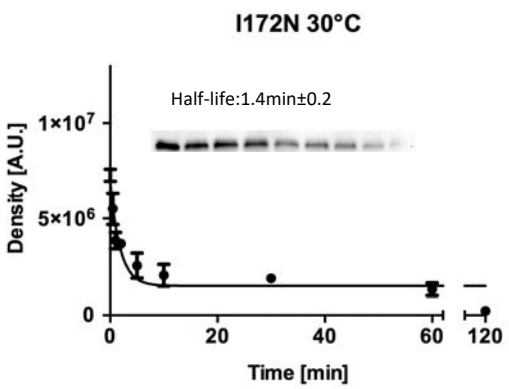
I172N 30°C
Half-life:1.4min±0.2
Density [A.U.]
1×10^7
5×10^6
0
0
20
40
60
120
Time [min]

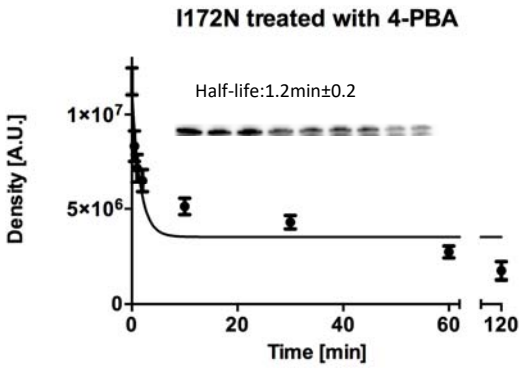
I172N treated with 4-PBA
Half-life:1.2min±0.2
Density [A.U.]
1×10^7
5×10^6
0
0
20
40
60
120
Time [min]

F

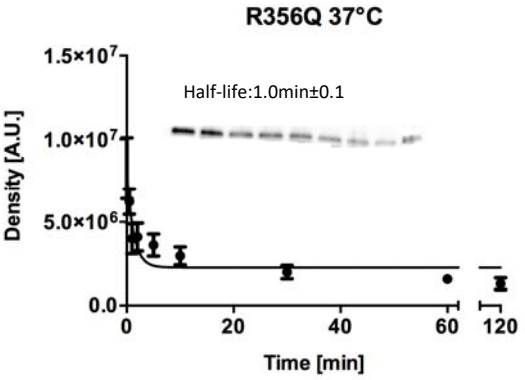
R356Q 37°C
Half-life:1.0min±0.1
Density [A.U.]
1.5×10^7
1.0×10^7
5.0×10^6
0.0
0
20
40
60
120
Time [min]

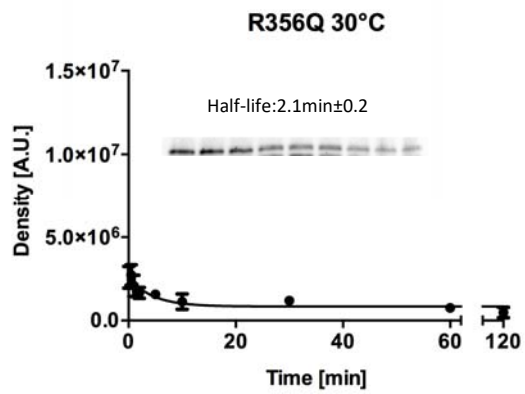
R356Q 30°C
Half-life:2.1min±0.2
Density [A.U.]
1.5×10^7
1.0×10^7
5.0×10^6
0.0
0
20
40
60
120
Time [min]

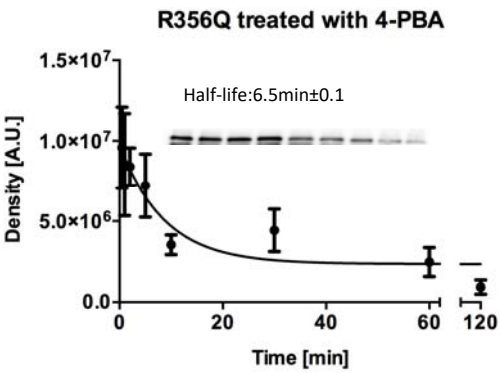
R356Q treated with 4-PBA
Half-life:6.5min±0.1
Density [A.U.]
1.5×10^7
1.0×10^7
5.0×10^6
0.0
0
20
40
60
120
Time [min]

G

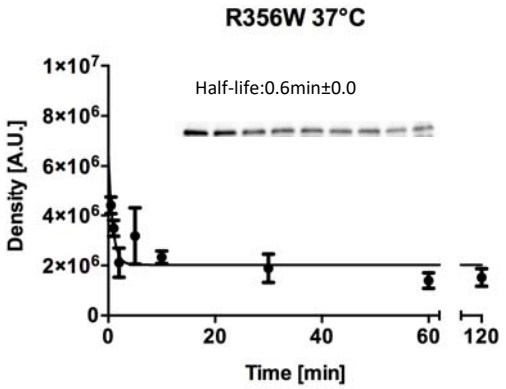
R356W 37°C
Half-life:0.6min±0.0
Density [A.U.]
Time [min]

H

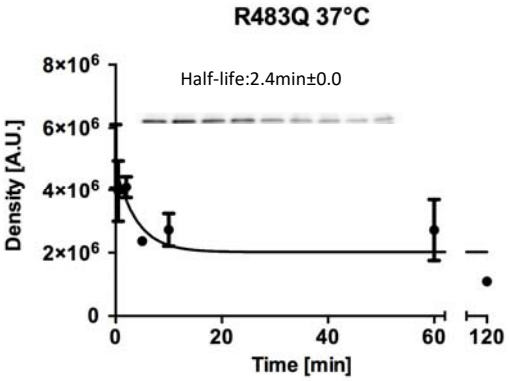
R483Q 37°C
Half-life:2.4min±0.0
Density [A.U.]
Time [min]

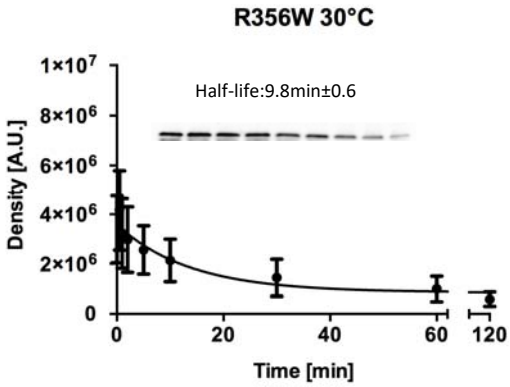
R356W 30°C
Half-life:9.8min±0.6
Density [A.U.]
Time [min]

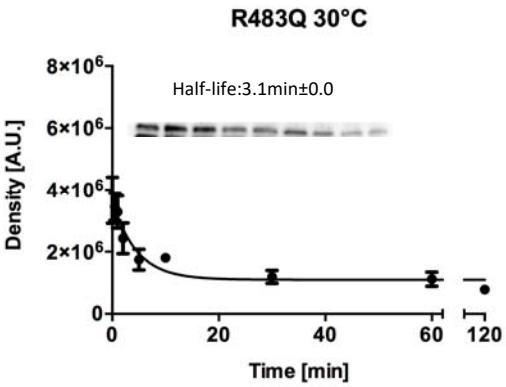
R483Q 30°C
Half-life:3.1min±0.0
Density [A.U.]
Time [min]

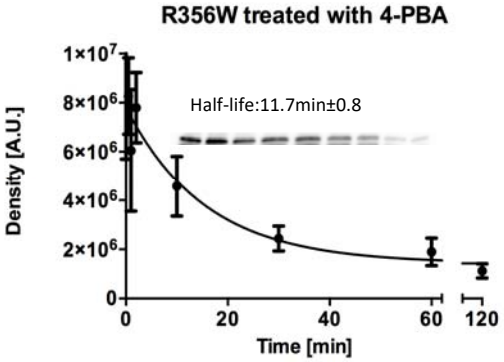
R356W treated with 4-PBA
Half-life:11.7min±0.8
Density [A.U.]
Time [min]

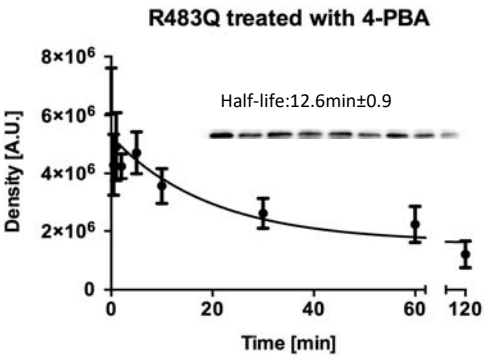
R483Q treated with 4-PBA
Half-life:12.6min±0.9
Density [A.U.]
Time [min]

I

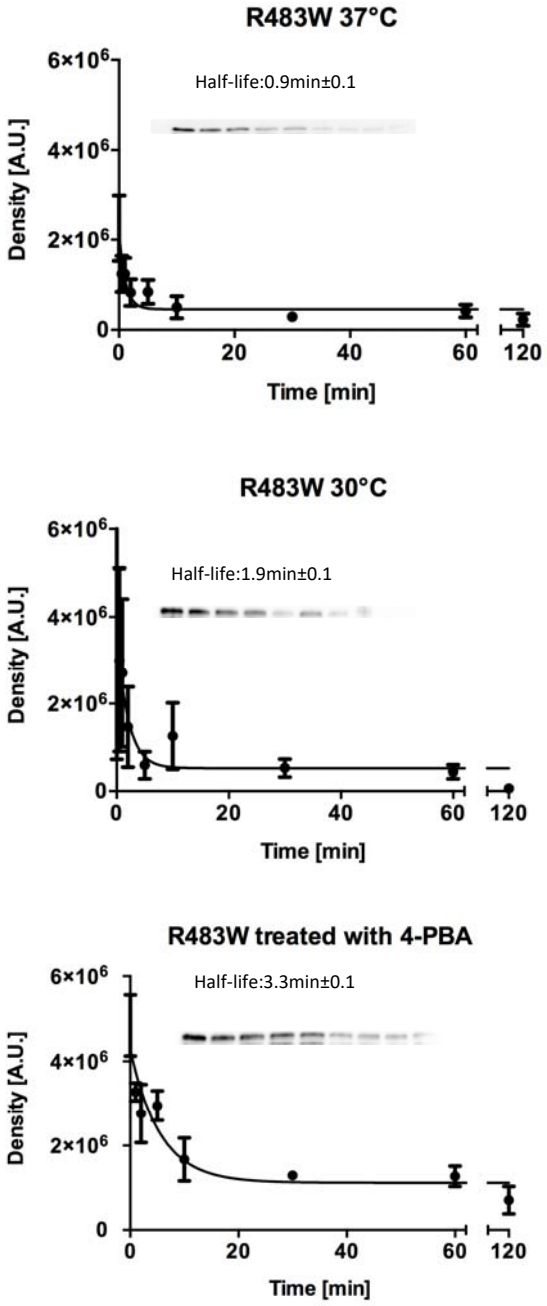

Figure 7 Effect of reduced temperature and 4-PBA on WT and variants CYP21A2 protein against limited proteolysis by proteinase K*. A to I columns represent degradation curves and representative western blot images of WT and variant proteins after treatment of 37°C, 30°C and 4-PBA respectively. CYP21A2 protein was detected with western blot immunoprecipitated from cell lysates as described in the materials and methods section and the blot shown was a representative fluorography from at least three independent experiments. Protein bands from the immunoblots were quantitated with Image J software. The values were expressed as percent of t = 0 chase time that was set to 100%. Error bars represented the standard error of mean from at least three independent experiments.*

Table 2 Effect of reduced temperature and 4-PBA on half-lives of WT and variant proteins

Mutation Protein variant	***37°C***	***30°C***	***P value***	***Untreated 37°C***	***4-PBA treated 37°C***	***P value***
WT	8.3 min±0.6	7.7 min±0.7	0.534	7.2 min±0.6	6.6 min±0.5	0.538
P30L	1.3 min±0.1	5.5 min±0.4	0.000	1.2 min±0.1	2.6 min±0.2	0.004
P30Q	0.9 min±0.1	8.0 min±0.8	0.001	0.8 min±0.1	1.3 min±0.1	0.016
G90V	0.9 min±0.2	5.9 min±0.4	0.000	0.6 min±0.0	5.4 min±0.2	0.000
I172N	1.4 min±0.2	1.4 min±0.2	0.979	1.6 min±0.2	1.2 min±0.2	0.297
V281G	2.4 min±0.1	2.8 min±0.1	0.063			
V281L	6.2 min±0.4	4.8 min±0.3	0.060			
D322G	3.8 min±0.2	2.9 min±0.6	0.191			
R356Q	1.0 min±0.1	2.1 min±0.2	0.009	1.0 min±0.1	6.5 min±0.1	0.000
R356W	0.6 min±0.0	9.8 min±0.6	0.004	0.6 min±0.0	11.7min±0.8	0.000
G375S	4.0 min±0.4	3.8 min±0.4	0.746			
P453S	5.7 min±0.5	6.5 min±0.6	0.369			
R483Q	2.4 min±0.0	3.1 min±0.0	0.000	2.3 min±0.2	12.6 min±0.9	0.000
R483W	0.9 min±0.1	1.9 min±0.1	0.012	0.9 min±0.1	3.3 min±0.1	0.000

5. Discussion

5.1 The correlations between protein half-lives and clinical phenotypes and molecular mechanisms

We studied protein degradation by investigating protein half-lives, to enhance the understanding of the molecular mechanism of 21-OHD. We chose 13 naturally occurring mutations in which we speculated from in *silico* modeling to be possibly related with protein instability. We investigated their susceptibility against proteinase K. We found that all variant proteins showed decreased stability to proteinase K compared with WT, suggesting that the instability speculating from the *in silico* modelling based on the crystal structure can be confirmed. Moreover, molecular characterization of *CYP21A2* protein variants can provide comprehensive structural explanations for clinical phenotype based on changes it brings in the structure of the protein (Haider et al., 2013). However, few functional studies have ever been performed to prove the structure-function relationship. Our results show for the first time that loss of half-lives of most variant proteins were in agreement with severity of the clinical phenotype. Different molecular mechanisms of each mutation that induce the structural instability and the correlation between protein half-life and phenotype are discussed below.

5.1.1 Impairment of hydrophobic interactions

Some residues have hydrophobic interactions with other residues from different structural elements to maintain the organization of secondary structures of protein. The mutations of these residues will disrupt the hydrophobic network and thus impair stability of the protein.

P30L and P30Q: In the present study, P30Q showed dramatically decrease of half-life shorter than 1min, and P30L had a longer half-life than P30Q, indicating that P30Q was less stable than P30L (Table 4). Patients with P30L and P30Q were found to present NC and SW phenotype respectively (Lajic et al., 1999; Tusie-Luna et al., 1991). Structural explanations for these two mutations are provided by crystal

structure. Since P30 is lodged in a hydrophobic cavity and help attach the P450 to the membrane, when substituted to the hydrophilic residue glutamine, it will cause a disruption of hydrophobic network disruption, induce steric conflicts with I59 and V70 (Figure 8A), and probably affect the flexibility of the tether between P450 and the membrane (Pallan, Lei, et al., 2015). When proline is substituted by leucine, another hydrophobic residue, it leads to less improper folding of the polypeptide and is better tolerated than glutamine, leading to milder form of 21-OHD (Haider et al., 2013). The half-life of P30Q in our study is compatible with the SW phenotype, but half-life of P30L is shorter than other variant proteins which had NC phenotype. Several functional studies showed that P30L caused only 40-70% loss of CYP21A2 enzyme activity *in vitro* and was related with the NC form (Marino et al., 2011). However, New et al. found that over 30% P30L-carrying patients presented with classical 21-OHD (M. I. New et al., 2013). Another study investigated the manifestation of patients with P30L mutation and found that compared with other NC patients, it produced more severe signs, including clitoromegaly (Tusie-Luna et al., 1991). Therefore, the spectrum of P30L is extremely wide. In addition, P30L may interfere with localization to the endoplasmic reticulum, which could have a further influence on the stability of enzyme than other NC variant proteins.

I172N: The phenotype of I172N is SV (Amor, Parker, Globerman, New, & White, 1988). The half-life of I172N in our study showed an obvious reduction but higher than those of SW variant proteins, which was consistent with the phenotype of I172N. Hsu et al. also used proteinase K to digest WT and I172N from yeast microsomes and found higher sensitivity of the I172N protein than WT toward proteinase K digestion (Hsu et al., 1996). I172 sits in helix E and is surrounded by M186 and M187 residues of F-helix. The isoleucine residue at the position of helix E is highly conserved and located in a hydrophobic pocket (Figure 8B). Substitution of the hydrophobic residue isoleucine to hydrophilic residue asparagine might disrupt the intramolecular hydrophobic interactions, leading the destabilizing of secondary structure of enzyme (Pallan, Lei, et al., 2015; White & Speiser, 2000).

V281L and V281G: Our experiment demonstrated that half-life of V281G was significantly shorter than that of WT, but longer than those of all SW proteins we measured, whereas that of V281L was slightly lower than WT, which in line with the phenotypes of V281L and V281G are NC and SV respectively (Lajic, Robins, Krone, Schwarz, & Wedell, 2001; Speiser, New, & White, 1988). V281 sits on the helix I and forms a hydrophobic patch together with helix H amino acids M258, M261, L262, and V265 (Figure 8C). When substituted from V to G, it will disrupt the interaction causing the impairment of protein stability. Moreover, the helix is also rendered unstable because of the high conformational flexibility imparted by glycine. When substituted to leucine, although increase in chain length leads to steric clashes, the influence on stability is relatively modest as leucine is a hydrophobic residue as well (Haider et al., 2013).

P453S: Only a slightly diminished half-life was shown in stability of P453S compared with WT, as expected of the mild clinical phenotype (Helmberg, Tusie-Luna, Tabarelli, Kofler, & White, 1992). P453 is positioned in a hydrophobic pocket surrounded by L308 (I-Helix), L452 (β8-sheet), L458 (β8-β9 loop). Proline is important for the secondary structure of this region due to the hydrophobic pocket where proline sits and the rigidity it introduces to the sharp turn (Figure 8D). Substitution to serine might disrupt hydrophobicity of this region and then misalign the sharp turn, resulting NC 21-OHD.

A B

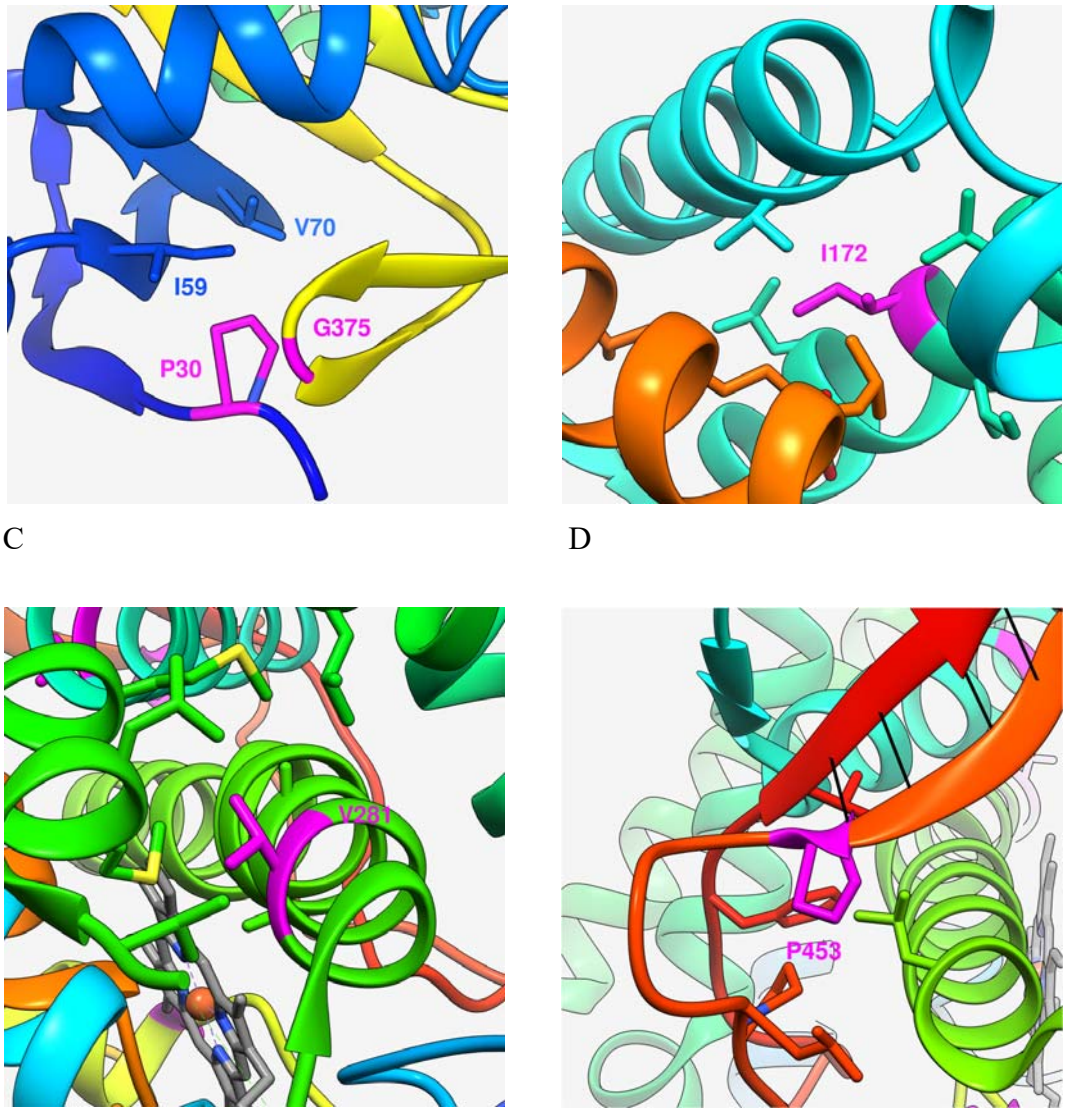

C D

Figure 8 Detailed local structural features of CYP21A2 variants which have impairment of hydrophobic interactions or introduction of bulkier residue*. (A) P30Q and G375S, (B) I172, (C) V281, and (D) P453. Residues are colored in magenta.*

5.1.2 Impairment of salt bridges and hydrogen bonds

In addition to hydrophobic network, CYP21A2 protein also has many salt bridges and hydrogen bonds which are crucial for the stability of tertiary structure of the enzyme. **D322G, R483Q, and R483W:** Like other SW variant proteins, R483W had the highest reduction in half-life. On the contrary, D322G and R483Q showed obviously higher stability than R483W. They are in line with their phenotypes (Bleicken et al., 2009; Kharrat et al., 2004; T. Robins et al., 2007; Stikkelbroeck et al., 2003). From

the crystal structures, R483 and D322 are related since there is a salt-bridge formation between them through the polar charged residues (Figure 9A). Therefore, when arginine is substituted to glutamine/tryptophan or aspartic acid is substituted to glycine, it will prevent the salt-bridge formation and subsequently affect stability of tertiary structure (Haider et al., 2013). Since tryptophan is nonpolar and uncharged residue, R483W may disrupt the salt-bridge completely and affect enzyme stability severely, so it is comprehensible that R483W leads to SW phenotype. On the contrary, glutamine and aspartic acid are both polar and uncharged residues and better tolerated than tryptophan, so D322G and R483Q cause milder phenotypes.

R356Q and R356W: The results of the present study clearly demonstrated that R356W showed the most severe instability while R356Q was less instable than R356W but still less stable than WT (Table 4). They are both in agreement with their clinical phenotypes. R356 (K-helix) forms a hydrogen bonding with Q389 (K'-helix) and Q462 (β8-β9). The hydrogen bonding plays a role in maintaining spatial configuration and tertiary structure of the CYP21A2 enzyme (Figure 9B) (Haider et al., 2013). When R356 is substituted to hydrophobic tryptophan, it will completely disrupt the hydrogen bonding, so that R356W exhibits SW 21-OHD. However, its substitution to hydrophilic glutamine, the hydrogen bonding is partly lost, resulting in SV 21-OHD.

G90V: The half-life of G90V we measured was rather short and compatible with the phenotype SW. G90 is located in B-B' loop adjacent to R91 (Figure 9C). The substitution of valine residue would indirectly introduce inflexibility to the loop through influence on hydrogen bond of R91 with the propionate side chains of heme, finally causing SW 21-OHD.

A

B

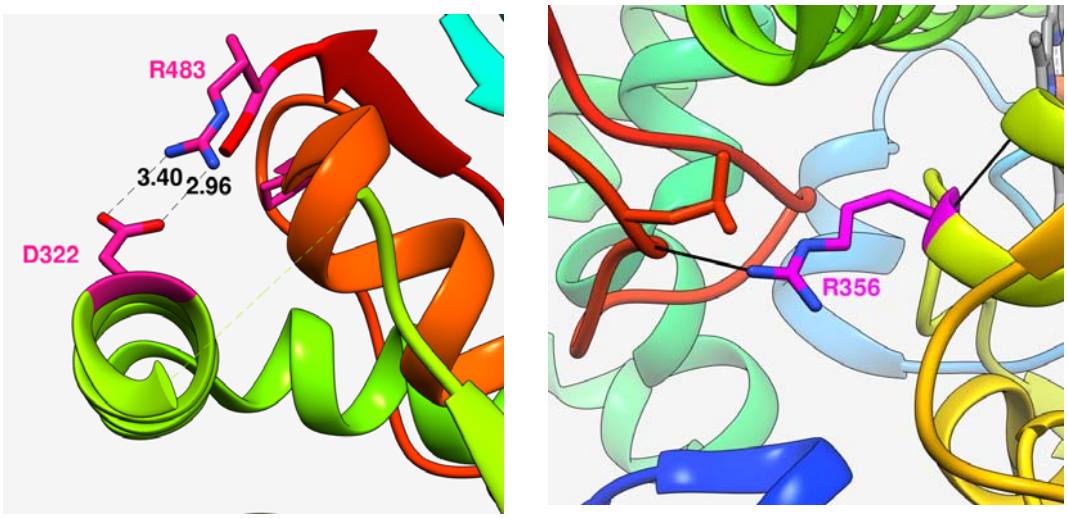

C

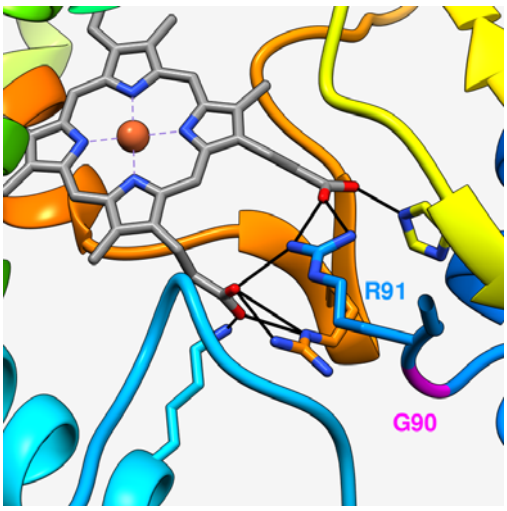

Figure 9 Detailed local structural features of CYP21A2 variants which have impairment of salt bridges and hydrogen bonds. *(A) D322 and R483, (B) R356, and (C) G90. Residues are colored in magenta.*

5.1.3 Introduction of bulkier residue

Protein instability also occurs when introduction of bulkier residues lead to destabilization of the secondary structure.

G375S: The phenotype of patients with G375S is SW (Lajic et al., 2002). However, the half-life (4.0min±0.6) we measure was not in agreement with the phenotype. It

was longer than all variant proteins of SW and SV and slightly lower than WT. Such an inconsistent result was also found in another study. Svetlana Lajićel al. also investigated half-life of G375S by blocking of translation using cycloheximide and analyzing proteins at different time points (0, 4, 8, 12, and 24 h) and found half-life of WT (13.0 h; minimum, 7.8 h; maximum, 23.6 h) has not great difference with that of G375S (10.7 h; minimum, 8.3 h; maximum, 14.1h), concluding that function of G375S was impaired more than overall structure (Lajic et al., 2002). The crystal structure reveals that G375 is present on the turn of β5-β6 hairpin. β5-β6 is only suitable for small residue. However, when substituted to serine, increased rigidity results in less conformational flexibility and hence reduces protein stability (Figure 8A).

In summary, most results of the present study are consistent with reported phenotypes, indicating good correlation between function and structure. Moreover, the location of CYP21A2 protein variants can provide a general understanding of structure-function relationship. However, there are still some exceptions, so we speculate that loss-of-function may be not always be explained by structure.

5.2 Role of reduced temperature and 4-PBA in protein stability

Importantly, our research demonstrated that stability of seven variant proteins can be enhanced by reduced temperature and chemical chaperone 4-PBA. It is the first time to explore reduced temperature and chemical chaperone as potential therapeutic tools for CYP21A2 protein variants *in vitro*. The results substantiate our hypothesis of protein misfolding with loss-of-function as a relevant molecular mechanism in 21-OHD that can be addressed by structural stabilization of CYP21A2 protein variants. Reduced temperature and 4-PBA have been applied in experiments with many different variant proteins and underlying mechanisms have been investigated.

5.2.1 Reduced temperature

It is long considered that protein folding and processing are temperature-sensitive (Powell & Zeitlin, 2002). In 1990, one study showed that, at reduced temperature

(19-33°C), H-2/beta 2-microglobulin complexes was promoted assembly, resulting in a high level of cell surface expression (Ljunggren et al., 1990). After that, increasing variant proteins have been confirmed as temperature-sensitive proteins. In order to explore the influence of reduced temperature on the protein synthesis, Heda and Marino investigated CFTR mRNA level at 27°C and found there was no increase (Heda & Marino, 2000). The molecular mechanisms of reduced temperature treatment are: (i) Reduced temperature helps the variant proteins escaping the ER quality control system so that degradation is inhibited. Such effect has been observed for α1-ATZ in CJZ12B cells. When the temperature was reduced from 37°C to 27°C, it was clear to see a significant decrease in degradation at 27°C by pulse-chase radio labeling (Burrows et al., 2000). A similar conclusion was obtained by some other studies in PrP^{187R} and V2R-V206D at low temperature (Gu & Singh, 2004; Robben et al., 2006). (ii) Lowering the temperature can contribute to partial folding of protein in the ER. Sharma el al. found at least some of the chains of ΔF508CFTR were properly assembled by the cellular machinery at reduced temperature (Sharma, Benharouga, Hu, & Lukacs, 2001). (iii) Reduced temperature also plays an important role in facilitating protein expression in targeted subcellular organelles. It has been shown that after incubation of ΔF508C127 cells at 27°C for 60h, biochemical and functional expression of ΔF508CFTR at the cell surface was increased (Heda & Marino, 2000). Some previous studies also have demonstrated that low temperature promotes some other disease-associated mutants such as PrPQ271R and PrP^{187} trafficking and functioning at the plasma membrane (Gu & Singh, 2004; Singh et al., 1997). As our experiment found, some variant proteins of CYP21A2 can be stabilized at 30°C, revealing that CYP21A2 protein is temperature-sensitive. We speculate that low temperature plays a vital role in reducing degradation, strengthening folding and increasing expression on ER membrane, but this needs further research.

5.2.2 Chemical chaperone 4-PBA

4-PBA has been shown in a number of studies that it can stabilize proteins that contain folding defects. Unlike reduced temperature, 4-PBA can enhance protein

expression. Heda and Marino demonstrated that 4-PBA can increase ΔF508 mRNA levels and protein expression (Heda & Marino, 2000). Similarly, another study also found that ABCA1 protein expression was increased via treatment with 4-PBA in all transfected cell lines (Sorrenson et al., 2013). Therefore, in our experiment, half-lives of R356W and R483Q are prolonged more than that of WT can be explained likely because of increased protein expression by 4-PBA treatment.

In addition, 4-PBA is believed to be of importance on prevention of aggregation of variant proteins, rescue of protein localization and restoration of functional proteins in many researches. By counting 293T cells bearing intracellular HFEC282Y aggregates, it was observed that after treated with 4-PBA, the percentage of cells with aggregates were remarkably decreased, which means that 4-PBA can prevent HFEC282Y aggregation (de Almeida et al., 2007).In studies of 4-PBA treatment on CFTR variant proteins responsible for cystic fibrosis, researchers have demonstrated that 4-PBA ameliorated ER retention and was sufficient to restore protein function *in vitro* and *in vivo* (R C Rubenstein et al., 1997; Zeitlin et al., 2002). The mechanism of 4-PBA function has been not completely understood; some studies thought it may act due to its effect on regulating cellular molecular chaperones. 4-PBA could downregulate protein and mRNA expression of the heat shock cognate protein HSC70 was observed in 4-PBA-treated IB3-1 cells (R. C. Rubenstein & Lyons, 2001). HSC70 is widely believed to take part in ubiquitin-dependent degradation of a number of intracellular proteins (Bercovich et al., 1997). Accordingly, 4-PBA can inhibit ubiquitination and subsequent degradation by the proteasomal system through inducing HSC70. Furthermore, there are a few studies that also found Hsp70 expression increasing after 4-PBA treatment (Choo-Kang & Zeitlin, 2001; Garcia-Bermejo et al., 1997; Gong, Zhang, Lam, Pang, & Yam, 2010). This could be beneficial for protein disaggregation, folding and complex remodeling, trafficking and maturation (Liberek, Lewandowska, & Zietkiewicz, 2008; Teter et al., 1999; Zhang et al., 2001; Zietkiewicz, Lewandowska, Stocki, & Liberek, 2006). As mentioned before, molecular chaperones also participate in the biogenesis of CYP21A2 protein. Although whether 4-PBA can

influence molecular chaperones is unclear, we could confirm that 4-PBA is beneficial for further processing of variant proteins.

Overall, some molecular mechanisms may be involved in actions of reduced temperature and chemical chaperone 4-PBA. However, the underlying molecular mechanisms of reduced temperature and 4-PBA on CYP21A2 variant proteins folding, disaggregation, trafficking and maturation, needs further investigation.

5.3 Mutation specific rescue of CYP21A2 variant proteins

The results of the present study clearly demonstrated that susceptibility to proteinase K of several variant proteins were not improved after reduced temperature and 4-PBA treatment, which illustrated that the rescue was not a general phenomenon but specific for a limited set of variant proteins. Robben el al. tested nine V2R mutants and found that treatment with chemical chaperones only rescued plasma membrane expression and increased receptor maturation of V2R-V206D (Robben et al., 2006). Similar results have been also shown in chemical chaperone treatment on HERG and CFTR mutants (Delisle et al., 2003; Sato, Ward, Krouse, Wine, & Kopito, 1996). The underlying mechanism is still unclear. From our results that all variant proteins from the same position (P30L and P30Q, R356Q and R356W, R483Q and R483W) were stabilized, we speculated that the ability to be rescued by temperature and chemical chaperones may be dependent upon the localization of residues in the protein structure of CYP21A2, but further studies are needed.

5.4 Perspective

Current experiments only investigated improvement of CYP21A2 protein variants stability but not activity by reduced temperature and chemical chaperone 4-PBA. Therefore, the next logical step it to measure enzyme activity to functionally characterize variant proteins and investigate the effect of reduced temperature and 4-PBA on activity. Furthermore, through comparison of enzyme stability and activity, a better understanding of its structure-function relationship can be achieved. We have

gained a few preliminary data on this aspect but this needs to be studied in future experiments.

As mentioned before, 4-PBA has been tested in Phase I clinical trials and oral administration of 4-PBA was well tolerated. These studied demonstrated that 4-PBA is a viable therapeutic approach for protein misfolding diseases (Burrows et al., 2000; R. C. Rubenstein & Zeitlin, 1998; Zeitlin et al., 2002). Thereby, further studies can investigate 4-PBA improvement on enzyme function and structure *in vivo* and subsequently phenotypes of patients.

Besides chemical chaperones inducing a stabilizing effect as non-specific binders, there are pharmacological chaperones which can selectively target variant proteins to achieve a more stable state. Pharmacological chaperones can provide molecular links or bridges to compensate for the loss of stabilizing interactions and introduction of destabilizing interactions caused by the mutation. Due to the characteristics of high specificity and affinity, pharmacological chaperones therapy becomes a developing area in the treatment of protein misfolding diseases arising from genetic mutations (Arakawa, Ejima, Kita, & Tsumoto, 2006; Ulloa-Aguirre, Janovick, Brothers, & Conn, 2004). Since unstable structure of CYP21A2 variant proteins was found in molecular modeling, pharmacological chaperones therapy may be a potential approach in the future. Identification of potential pharmacological chaperones are firstly required by high-throughput screening and rational design, and then enzyme stability and activity can be tested in cell models treated with selected pharmacological chaperones. It would be a long term task but extremely rewarding for 21-OHD treatment with the least risk of side effects if successful.

6. Summary-Zusammenfassung

Congenital adrenal hyperplasia (CAH) is a group of autosomal recessive disorders characterized by impaired synthesis of cortisol. 21-hydroxylase deficiency (21-OHD), the most common form of CAH, is caused by defects of the *CYP21A2* gene and constitutes a life-threatening disease. Patients with 21-OHD experience significant health concerns due to co-morbidities which are often treatment-related. Therefore current treatment strategies, which consist of steroid replacement, are unsatisfying. New causative treatment options with the least risk of side effects are needed.

Based on the research of other diseases investigating protein misfolding as underlying pathophysiological mechanism such as cystic fibrosis or phenylketonuria, we hypothesize that also 21-OHD in part is a protein misfolding disease. *In silico* modelling suggested protein instability and misfolding to play a significant role in the pathogenesis of 21-OHD. Thus, in this research, we investigated 13 variant proteins which are caused by point mutations and speculated from *in silico* modelling to be related with impaired protein stability. The selected variant proteins cover all three phenotypes of 21-OHD and do not cause direct disruption of heme and/or substrate binding. The influence of 4-PBA and reduced temperature on variant protein half-life (susceptibility to proteinase K) was investigated. We found that all variant proteins showed reduced half-lives compared with WT, indicating that CYP21A2 variant enzymes were more susceptible to degradation by protease K. Reduced temperature and 4-PBA could stabilize some but not all variant proteins, which illustrated that the rescue was not a general phenomenon but specific for a limited set of variant proteins. There were seven variant proteins P30L, P30Q, G90V, R356Q, R356W, R483Q and R483W which could be stabilized by both approaches.

Our data substantiated the hypothesis of protein instability as a relevant molecular mechanism in 21-OHD that can be addressed by structural stabilization of CYP21A2 variant protein. These strategies above may provide new avenues in 21-OHD treatment in the future.

Das Adrenogenitale Syndrom (AGS) ist eine Gruppe autosomal-rezessiver Erkrankungen, die durch die beeinträchtige Synthese von Cortisol gekennzeichnet ist. Der 21-Hydroxylase-Mangel (21-OHD), die häufigste Form des AGS, beruht auf einem Defekt des *CYP21A2*-Gens, was zu einer lebensbedrohlichen Krankheit führt. Patienten mit 21-OHD sind von erheblichen gesundheitlichen Problemen betroffen, die oftmals als Begleiterkrankungen durch die Therapie auftreten. Die aktuell zur Behandlung eingesetzte Hormonersatztherapie ist somit nicht zufriedenstellend. Es werden neue kausale Therapieansätze mit einem geringeren Risiko für Nebenwirkungen benötigt.

Basierend auf Forschungsarbeiten anderer Erkrankungen wie der zystischen Fibrose oder Phenylketonurie, bei welchen Proteinfehlfaltung als zugrundeliegender Pathomechanismus eine wichtige Rolle spielt, hat diese Arbeit die Hypothese, dass auch der 21-OHD zum Teil durch Proteinfehlfaltung bedingt ist. In einem *in silico* Modell untersuchten wir, ob Proteininstabilität und Fehlfaltung eine entscheidende Rolle in der Pathogenese des 21-OHD spielen könnte. Folglich werden in dieser Forschungsarbeit 13 verschiedene Proteinvarianten untersucht, die auf Grund des *in silico* Modells mit einer verminderten Proteinstabilität in Verbindung gebracht werden können. Die ausgewählten Proteinvarianten, schließen zum einen alle drei Phänotypen des 21-OHD mit ein, zum anderen unterbrechen sie nicht die Bindung des Häms und/oder des Substrats. Der Einfluss von 4PBA und einer verminderten Temperatur auf die Halbwertszeit der verschiedenen Varianten des Proteins (Suszeptibilität gegenüber Proteinase K) wurde untersucht. Wir haben herausgefunden, dass alle Proteinvarianten im Vergleich zum Wildtyp eine verminderte Halbwertszeit zeigten, was darauf hinweist, dass die CYP21A2 Enzymvarianten anfälliger für den Abbau durch Proteinase K waren. Eine verringerte Temperatur und 4-PBA konnte manche, aber nicht alle der Proteinvarianten stabilisieren, wodurch gezeigt wurde, dass die Stabilisierung nicht ein generelles Phänomen, sondern nur spezifisch auf eine begrenzte Zahl der Proteinvarianten zutraf. Es gab sieben verschiedene

Proteinvarianten, P30L, P30Q, G90V, R356Q, R356W, R483Q und R483W, die durch beide Methoden stabilisiert werden konnten.

Unsere Daten untermauern die Hypothese der Proteinstabilität als relevanter molekularer Mechanismus des 21-OHD, dem mit einer strukturellen Stabilisierung des CYP21A2 begegnet werden kann. Diese Strategien könnten neue Wege für die zukünftige Behandlung des 21-OHD darstellen.

7. References

Acharya, P., Liao, M., Engel, J. C., & Correia, M. A. (2011). Liver cytochrome P450 3A endoplasmic reticulum-associated degradation: a major role for the p97 AAA ATPase in cytochrome P450 3A extraction into the cytosol. *J Biol Chem, 286*(5), 3815-3828. doi:10.1074/jbc.M110.186981

Amor, M., Parker, K. L., Globerman, H., New, M. I., & White, P. C. (1988). Mutation in the CYP21B gene (Ile-172----Asn) causes steroid 21-hydroxylase deficiency. *Proc Natl Acad Sci U S A, 85*(5), 1600-1604.

Arakawa, T., Ejima, D., Kita, Y., & Tsumoto, K. (2006). Small molecule pharmacological chaperones: From thermodynamic stabilization to pharmaceutical drugs. *Biochim Biophys Acta, 1764*(11), 1677-1687. doi:10.1016/j.bbapap.2006.08.012

Aridor, M. (2007). Visiting the ER: the endoplasmic reticulum as a target for therapeutics in traffic related diseases. *Adv Drug Deliv Rev, 59*(8), 759-781. doi:10.1016/j.addr.2007.06.002

Aruffo, A. (2001). Transient expression of proteins using COS cells. *Curr Protoc Neurosci, Chapter 4*, Unit 4.7. doi:10.1002/0471142301.ns0407s02

Bercovich, B., Stancovski, I., Mayer, A., Blumenfeld, N., Laszlo, A., Schwartz, A. L., & Ciechanover, A. (1997). Ubiquitin-dependent degradation of certain protein substrates in vitro requires the molecular chaperone Hsc70. *J Biol Chem, 272*(14), 9002-9010.

Blanchong, C. A., Zhou, B., Rupert, K. L., Chung, E. K., Jones, K. N., Sotos, J. F., . . . Yung Yu, C. (2000). Deficiencies of human complement component C4A and C4B and heterozygosity in length variants of RP-C4-CYP21-TNX (RCCX) modules in caucasians. The load of RCCX genetic diversity on major histocompatibility complex-associated disease. *J Exp Med, 191*(12), 2183-2196.

Bleicken, C., Loidi, L., Dhir, V., Parajes, S., Quinteiro, C., Dominguez, F., . . . Krone, N. (2009). Functional characterization of three CYP21A2 sequence variants (p.A265V, p.W302S, p.D322G) employing a yeast co-expression system. *Hum Mutat, 30*(2), E443-450. doi:10.1002/humu.20926

Bonfig, W., Bechtold, S., Schmidt, H., Knorr, D., & Schwarz, H. P. (2007). Reduced final height outcome in congenital adrenal hyperplasia under prednisone treatment: deceleration of growth velocity during puberty. *J Clin Endocrinol Metab, 92*(5), 1635-1639. doi:10.1210/jc.2006-2109

Bradford, M. M. (1976). A rapid and sensitive method for the quantitation of microgram quantities of protein utilizing the principle of protein-dye binding. *Anal Biochem, 72*, 248-254.

Burrows, J. A., Willis, L. K., & Perlmutter, D. H. (2000). Chemical chaperones mediate increased secretion of mutant alpha 1-antitrypsin (alpha 1-AT) Z: A potential pharmacological strategy for prevention of liver injury and emphysema in alpha 1-AT deficiency. *Proc Natl Acad Sci U S A, 97*(4), 1796-1801.

Carroll, M. C., Campbell, R. D., & Porter, R. R. (1985). Mapping of steroid 21-hydroxylase genes adjacent to complement component C4 genes in HLA, the major histocompatibility complex in man. *Proc Natl Acad Sci U S A, 82*(2), 521-525.

Chapman, E., Fry, A. N., & Kang, M. (2011). The complexities of p97 function in health and disease. *Mol Biosyst, 7*(3), 700-710. doi:10.1039/c0mb00176g

Chiou, S. H., Hu, M. C., & Chung, B. C. (1990). A missense mutation at Ile172----Asn or Arg356----Trp causes steroid 21-hydroxylase deficiency. *J Biol Chem, 265*(6), 3549-3552.

Choo-Kang, L. R., & Zeitlin, P. L. (2001). Induction of HSP70 promotes DeltaF508 CFTR trafficking. *Am J*

Physiol Lung Cell Mol Physiol, 281(1), L58-68.

Collins, A. F., Pearson, H. A., Giardina, P., McDonagh, K. T., Brusilow, S. W., & Dover, G. J. (1995). Oral sodium phenylbutyrate therapy in homozygous beta thalassemia: a clinical trial. *Blood, 85*(1), 43-49.

Correia, M. A., & Liao, M. (2007). Cellular proteolytic systems in P450 degradation: evolutionary conservation from Saccharomyces cerevisiae to mammalian liver. *Expert Opin Drug Metab Toxicol, 3*(1), 33-49. doi:10.1517/17425255.3.1.33

Cuisset, L., Tichonicky, L., Jaffray, P., & Delpech, M. (1997). The effects of sodium butyrate on transcription are mediated through activation of a protein phosphatase. *J Biol Chem, 272*(39), 24148-24153.

D'Anna, J. A., Tobey, R. A., & Gurley, L. R. (1980). Concentration-dependent effects of sodium butyrate in Chinese hamster cells: cell-cycle progression, inner-histone acetylation, histone H1 dephosphorylation, and induction of an H1-like protein. *Biochemistry, 19*(12), 2656-2671.

de Almeida, S. F., Picarote, G., Fleming, J. V., Carmo-Fonseca, M., Azevedo, J. E., & de Sousa, M. (2007). Chemical chaperones reduce endoplasmic reticulum stress and prevent mutant HFE aggregate formation. *J Biol Chem, 282*(38), 27905-27912. doi:10.1074/jbc.M702672200

Delisle, B. P., Anderson, C. L., Balijepalli, R. C., Anson, B. D., Kamp, T. J., & January, C. T. (2003). Thapsigargin selectively rescues the trafficking defective LQT2 channels G601S and F805C. *J Biol Chem, 278*(37), 35749-35754. doi:10.1074/jbc.M305787200

Ellgaard, L., & Helenius, A. (2003). Quality control in the endoplasmic reticulum. *Nat Rev Mol Cell Biol, 4*(3), 181-191. doi:10.1038/nrm1052

Fontana, A., de Laureto, P. P., Spolaore, B., Frare, E., Picotti, P., & Zambonin, M. (2004). Probing protein structure by limited proteolysis. *Acta Biochim Pol, 51*(2), 299-321. doi:035001299

French, P. J., van Doorninck, J. H., Peters, R. H., Verbeek, E., Ameen, N. A., Marino, C. R., . . . Scholte, B. J. (1996). A delta F508 mutation in mouse cystic fibrosis transmembrane conductance regulator results in a temperature-sensitive processing defect in vivo. *J Clin Invest, 98*(6), 1304-1312. doi:10.1172/JCI118917

Garcia-Bermejo, L., Vilaboa, N. E., Perez, C., Galan, A., De Blas, E., & Aller, P. (1997). Modulation of heat-shock protein 70 (HSP70) gene expression by sodium butyrate in U-937 promonocytic cells: relationships with differentiation and apoptosis. *Exp Cell Res, 236*(1), 268-274. doi:10.1006/excr.1997.3725

Gersting, S. W., Kemter, K. F., Staudigl, M., Messing, D. D., Danecka, M. K., Lagler, F. B., . . . Muntau, A. C. (2008). Loss of function in phenylketonuria is caused by impaired molecular motions and conformational instability. *Am J Hum Genet, 83*(1), 5-17. doi:10.1016/j.ajhg.2008.05.013

Gluzman, Y. (1981). SV40-transformed simian cells support the replication of early SV40 mutants. *Cell, 23*(1), 175-182.

Gong, B., Zhang, L. Y., Lam, D. S., Pang, C. P., & Yam, G. H. (2010). Sodium 4-phenylbutyrate ameliorates the effects of cataract-causing mutant gammaD-crystallin in cultured cells. *Mol Vis, 16*, 997-1003.

Gu, Y., & Singh, N. (2004). Doxycycline and protein folding agents rescue the abnormal phenotype of familial CJD H187R in a cell model. *Brain Res Mol Brain Res, 123*(1-2), 37-44. doi:10.1016/j.molbrainres.2004.01.006

Haider, S., Islam, B., D'Atri, V., Sgobba, M., Poojari, C., Sun, L., . . . New, M. I. (2013). Structure-phenotype correlations of human CYP21A2 mutations in congenital adrenal

hyperplasia. *Proc Natl Acad Sci U S A, 110*(7), 2605-2610. doi:10.1073/pnas.1221133110

Hargitai, G., Sólyom, J., Battelino, T., Lebl, J., Pribilincová, Z., Hauspie, R., . . . Group, M.-C. S. (2001). Growth patterns and final height in congenital adrenal hyperplasia due to classical 21-hydroxylase deficiency. Results of a multicenter study. *Horm Res, 55*(4), 161-171. doi:49990

Heda, G. D., & Marino, C. R. (2000). Surface expression of the cystic fibrosis transmembrane conductance regulator mutant DeltaF508 is markedly upregulated by combination treatment with sodium butyrate and low temperature. *Biochem Biophys Res Commun, 271*(3), 659-664. doi:10.1006/bbrc.2000.2684

Helmberg, A., Tusie-Luna, M. T., Tabarelli, M., Kofler, R., & White, P. C. (1992). R339H and P453S: CYP21 mutations associated with nonclassic steroid 21-hydroxylase deficiency that are not apparent gene conversions. *Mol Endocrinol, 6*(8), 1318-1322. doi:10.1210/mend.6.8.1406709

Higashi, Y., Yoshioka, H., Yamane, M., Gotoh, O., & Fujii-Kuriyama, Y. (1986). Complete nucleotide sequence of two steroid 21-hydroxylase genes tandemly arranged in human chromosome: a pseudogene and a genuine gene. *Proc Natl Acad Sci U S A, 83*(9), 2841-2845.

Hsu, L. C., Hsu, N. C., Guzova, J. A., Guzov, V. M., Chang, S. F., & Chung, B. C. (1996). The common I172N mutation causes conformational change of cytochrome P450c21 revealed by systematic mutation, kinetic, and structural studies. *J Biol Chem, 271*(6), 3306-3310.

Kelly, J. W., & Balch, W. E. (2006). The integration of cell and chemical biology in protein folding. *Nat Chem Biol, 2*(5), 224-227. doi:10.1038/nchembio0506-224

Kharrat, M., Tardy, V., M'Rad, R., Maazoul, F., Jemaa, L. B., Refai, M., . . . Chaabouni, H. (2004). Molecular genetic analysis of Tunisian patients with a classic form of 21-hydroxylase deficiency: identification of four novel mutations and high prevalence of Q318X mutation. *J Clin Endocrinol Metab, 89*(1), 368-374. doi:10.1210/jc.2003-031056

Klehr, D., Schlake, T., Maass, K., & Bode, J. (1992). Scaffold-attached regions (SAR elements) mediate transcriptional effects due to butyrate. *Biochemistry, 31*(12), 3222-3229.

Koppens, P. F. J., Hoogenboezem, T., & Degenhart, H. J. (2002). Carriership of a defective tenascin-X gene in steroid 21-hydroxylase deficiency patients: TNXB -TNXA hybrids in apparent large-scale gene conversions. *Hum Mol Genet, 11*(21), 2581-2590.

Krone, N., Braun, A., Roscher, A. A., Knorr, D., & Schwarz, H. P. (2000). Predicting phenotype in steroid 21-hydroxylase deficiency? Comprehensive genotyping in 155 unrelated, well defined patients from southern Germany. *J Clin Endocrinol Metab, 85*(3), 1059-1065. doi:10.1210/jcem.85.3.6441

Lajic, S., Clauin, S., Robins, T., Vexiau, P., Blanche, H., Bellanne-Chantelot, C., & Wedell, A. (2002). Novel mutations in CYP21 detected in individuals with hyperandrogenism. *J Clin Endocrinol Metab, 87*(6), 2824-2829. doi:10.1210/jcem.87.6.8525

Lajic, S., Levo, A., Nikoshkov, A., Lundberg, Y., Partanen, J., & Wedell, A. (1997). A cluster of missense mutations at Arg356 of human steroid 21-hydroxylase may impair redox partner interaction. *Hum Genet, 99*(6), 704-709.

Lajic, S., Nikoshkov, A., Holst, M., & Wedell, A. (1999). Effects of missense mutations and deletions on membrane anchoring and enzyme function of human steroid 21-hydroxylase (P450c21). *Biochem Biophys Res Commun, 257*(2), 384-390. doi:10.1006/bbrc.1999.0482

Lajic, S., Robins, T., Krone, N., Schwarz, H. P., & Wedell, A. (2001). CYP21 mutations in simple virilizing congenital adrenal hyperplasia. *J Mol Med (Berl), 79*(10), 581-586.

doi:10.1007/s001090100261

Lambert, G., Becker, B., Schreiber, R., Boucherot, A., Reth, M., & Kunzelmann, K. (2001). Control of cystic fibrosis transmembrane conductance regulator expression by BAP31. *J Biol Chem, 276*(23), 20340-20345. doi:10.1074/jbc.M011209200

Lee, M. C. S., Miller, E. A., Goldberg, J., Orci, L., & Schekman, R. (2004). Bi-directional protein transport between the ER and Golgi. *Annu Rev Cell Dev Biol, 20*, 87-123. doi:10.1146/annurev.cellbio.20.010403.105307

Liao, M., Faouzi, S., Karyakin, A., & Correia, M. A. (2006). Endoplasmic reticulum-associated degradation of cytochrome P450 CYP3A4 in Saccharomyces cerevisiae: further characterization of cellular participants and structural determinants. *Mol Pharmacol, 69*(6), 1897-1904. doi:10.1124/mol.105.021816

Liberek, K., Lewandowska, A., & Zietkiewicz, S. (2008). Chaperones in control of protein disaggregation. *EMBO J, 27*(2), 328-335. doi:10.1038/sj.emboj.7601970

Ljunggren, H. G., Stam, N. J., Ohlen, C., Neefjes, J. J., Hoglund, P., Heemels, M. T., . . . et al. (1990). Empty MHC class I molecules come out in the cold. *Nature, 346*(6283), 476-480. doi:10.1038/346476a0

Loidi, L., Quinteiro, C., Parajes, S., Barreiro, J., Leston, D. G., Cabezas-Agricola, J. M., . . . Dominguez, F. (2006). High variability in CYP21A2 mutated alleles in Spanish 21-hydroxylase deficiency patients, six novel mutations and a founder effect. *Clin Endocrinol (Oxf), 64*(3), 330-336. doi:10.1111/j.1365-2265.2006.02465.x

Maestri, N. E., Brusilow, S. W., Clissold, D. B., & Bassett, S. S. (1996). Long-term treatment of girls with ornithine transcarbamylase deficiency. *N Engl J Med, 335*(12), 855-859. doi:10.1056/nejm199609193351204

Marino, R., Ramirez, P., Galeano, J., Perez Garrido, N., Rocco, C., Ciaccio, M., . . . Belgorosky, A. (2011). Steroid 21-hydroxylase gene mutational spectrum in 454 Argentinean patients: genotype-phenotype correlation in a large cohort of patients with congenital adrenal hyperplasia. *Clin Endocrinol (Oxf), 75*(4), 427-435. doi:10.1111/j.1365-2265.2011.04123.x

McCracken, A. A., & Brodsky, J. L. (2005). Recognition and delivery of ERAD substrates to the proteasome and alternative paths for cell survival. *Curr Top Microbiol Immunol, 300*, 17-40.

Merke, D. P., & Bornstein, S. R. (2005). Congenital adrenal hyperplasia. *The Lancet, 365*(9477), 2125-2136. doi:10.1016/s0140-6736(05)66736-0

Miller, J., & Gordon, C. (2005). The regulation of proteasome degradation by multi-ubiquitin chain binding proteins. *FEBS Lett, 579*(15), 3224-3230. doi:10.1016/j.febslet.2005.03.042

Miller, W. L. (2009). Androgen synthesis in adrenarche. *Rev Endocr Metab Disord, 10*(1), 3-17. doi:10.1007/s11154-008-9102-4

Minutolo, C., Nadra, A. D., Fernandez, C., Taboas, M., Buzzalino, N., Casali, B., . . . Dain, L. (2011). Structure-based analysis of five novel disease-causing mutations in 21-hydroxylase-deficient patients. *PLoS One, 6*(1), e15899. doi:10.1371/journal.pone.0015899

Morishima, Y., Peng, H. M., Lin, H. L., Hollenberg, P. F., Sunahara, R. K., Osawa, Y., & Pratt, W. B. (2005). Regulation of cytochrome P450 2E1 by heat shock protein 90-dependent stabilization and CHIP-dependent proteasomal degradation. *Biochemistry, 44*(49), 16333-16340. doi:10.1021/bi0515570

Mornet, E., & Gibrat, J. F. (2000). A 3D model of human P450c21: study of the putative effects of steroid 21-hydroxylase gene mutations. *Hum Genet, 106*(3), 330-339.

New, M. I. (2006). Extensive clinical experience: nonclassical 21-hydroxylase deficiency. *J Clin Endocrinol Metab, 91*(11), 4205-4214. doi:10.1210/jc.2006-1645

New, M. I., Abraham, M., Gonzalez, B., Dumic, M., Razzaghy-Azar, M., Chitayat, D., . . . Yuen, T. (2013). Genotype-phenotype correlation in 1,507 families with congenital adrenal hyperplasia owing to 21-hydroxylase deficiency. *Proc Natl Acad Sci U S A, 110*(7), 2611-2616. doi:10.1073/pnas.1300057110

Nikoshkov, A., Lajic, S., Holst, M., Wedell, A., & Luthman, H. (1997). Synergistic effect of partially inactivating mutations in steroid 21-hydroxylase deficiency. *J Clin Endocrinol Metab, 82*(1), 194-199. doi:10.1210/jcem.82.1.3678

Nunez, B. S., Lobato, M. N., White, P. C., & Meseguer, A. (1999). Functional analysis of four CYP21 mutations from spanish patients with congenital adrenal hyperplasia. *Biochem Biophys Res Commun, 262*(3), 635-637. doi:10.1006/bbrc.1999.1271

Owerbach, D., Sherman, L., Ballard, A. L., & Azziz, R. (1992). Pro-453 to Ser mutation in CYP21 is associated with nonclassic steroid 21-hydroxylase deficiency. *Mol Endocrinol, 6*(8), 1211-1215. doi:10.1210/mend.6.8.1406699

Pallan, P. S., Lei, L., Wang, C., Waterman, M. R., Guengerich, F. P., & Egli, M. (2015). Research Resource: Correlating Human Cytochrome P450 21A2 Crystal Structure and Phenotypes of Mutations in Congenital Adrenal Hyperplasia. *Mol Endocrinol, 29*(9), 1375-1384. doi:10.1210/ME.2015-1127

Pallan, P. S., Wang, C., Lei, L., Yoshimoto, F. K., Auchus, R. J., Waterman, M. R., . . . Egli, M. (2015). Human Cytochrome P450 21A2, the Major Steroid 21-Hydroxylase: STRUCTURE OF THE ENZYME.PROGESTERONE SUBSTRATE COMPLEX AND RATE-LIMITING C-H BOND CLEAVAGE. *J Biol Chem, 290*(21), 13128-13143. doi:10.1074/jbc.M115.646307

Pang, S. (2003). Newborn screening for congenital adrenal hyperplasia. *Pediatr Ann, 32*(8), 516-523.

Park, S. H., Bolender, N., Eisele, F., Kostova, Z., Takeuchi, J., Coffino, P., & Wolf, D. H. (2007). The cytoplasmic Hsp70 chaperone machinery subjects misfolded and endoplasmic reticulum import-incompetent proteins to degradation via the ubiquitin-proteasome system. *Mol Biol Cell, 18*(1), 153-165. doi:10.1091/mbc.E06-04-0338

Perlmutter, D. H. (2002). Chemical chaperones: a pharmacological strategy for disorders of protein folding and trafficking. *Pediatr Res, 52*(6), 832-836. doi:10.1203/00006450-200212000-00004

Powell, K., & Zeitlin, P. L. (2002). Therapeutic approaches to repair defects in deltaF508 CFTR folding and cellular targeting. *Adv Drug Deliv Rev, 54*(11), 1395-1408.

Rainey, W. E., Carr, B. R., Sasano, H., Suzuki, T., & Mason, J. I. (2002). Dissecting human adrenal androgen production. *Trends Endocrinol Metab, 13*(6), 234-239.

Reisch, N., Arlt, W., & Krone, N. (2011). Health problems in congenital adrenal hyperplasia due to 21-hydroxylase deficiency. *Horm Res Paediatr, 76*(2), 73-85. doi:10.1159/000327794

Reisch, N., Rottenkolber, M., Greifenstein, A., Krone, N., Schmidt, H., Reincke, M., . . . Beuschlein, F. (2013). Testicular adrenal rest tumors develop independently of long-term disease control: a longitudinal analysis of 50 adult men with congenital adrenal hyperplasia due to classic 21-hydroxylase deficiency. *J Clin Endocrinol Metab, 98*(11), E1820-1826. doi:10.1210/jc.2012-3181

Resar, L. M. S., Segal, J. B., Fitzpatric, L. K., Friedmann, A., Brusilow, S. W., & Dover, G. J. (2002). Induction of fetal hemoglobin synthesis in children with sickle cell anemia on low-dose oral sodium phenylbutyrate therapy. *J Pediatr Hematol Oncol, 24*(9), 737-741.

Robben, J. H., Sze, M., Knoers, N. V. A. M., & Deen, P. M. T. (2006). Rescue of vasopressin V2 receptor mutants by chemical chaperones: specificity and mechanism. *Mol Biol Cell, 17*(1), 379-386. doi:10.1091/mbc.E05-06-0579

Robins, T., Bellanne-Chantelot, C., Barbaro, M., Cabrol, S., Wedell, A., & Lajic, S. (2007). Characterization of novel missense mutations in CYP21 causing congenital adrenal hyperplasia. *J Mol Med (Berl), 85*(3), 247-255. doi:10.1007/s00109-006-0121-x

Robins, T., Carlsson, J., Sunnerhagen, M., Wedell, A., & Persson, B. (2006). Molecular model of human CYP21 based on mammalian CYP2C5: structural features correlate with clinical severity of mutations causing congenital adrenal hyperplasia. *Mol Endocrinol, 20*(11), 2946-2964. doi:10.1210/me.2006-0172

Rubenstein, R. C., Egan, M. E., & Zeitlin, P. L. (1997). In vitro pharmacologic restoration of CFTR-mediated chloride transport with sodium 4-phenylbutyrate in cystic fibrosis epithelial cells containing delta F508-CFTR. *J Clin Invest, 100*(10), 2457-2465. doi:10.1172/jci119788

Rubenstein, R. C., & Lyons, B. M. (2001). Sodium 4-phenylbutyrate downregulates HSC70 expression by facilitating mRNA degradation. *Am J Physiol Lung Cell Mol Physiol, 281*(1), L43-51.

Rubenstein, R. C., & Zeitlin, P. L. (1998). A pilot clinical trial of oral sodium 4-phenylbutyrate (Buphenyl) in deltaF508-homozygous cystic fibrosis patients: partial restoration of nasal epithelial CFTR function. *Am J Respir Crit Care Med, 157*(2), 484-490. doi:10.1164/ajrccm.157.2.9706088

Sato, S., Ward, C. L., Krouse, M. E., Wine, J. J., & Kopito, R. R. (1996). Glycerol reverses the misfolding phenotype of the most common cystic fibrosis mutation. *J Biol Chem, 271*(2), 635-638.

Sharma, M., Benharouga, M., Hu, W., & Lukacs, G. L. (2001). Conformational and temperature-sensitive stability defects of the delta F508 cystic fibrosis transmembrane conductance regulator in post-endoplasmic reticulum compartments. *J Biol Chem, 276*(12), 8942-8950. doi:10.1074/jbc.M009172200

Shimizu, Y., Okuda-Shimizu, Y., & Hendershot, L. M. (2010). Ubiquitylation of an ERAD substrate occurs on multiple types of amino acids. *Mol Cell, 40*(6), 917-926. doi:10.1016/j.molcel.2010.11.033

Singh, N., Zanusso, G., Chen, S. G., Fujioka, H., Richardson, S., Gambetti, P., & Petersen, R. B. (1997). Prion protein aggregation reverted by low temperature in transfected cells carrying a prion protein gene mutation. *J Biol Chem, 272*(45), 28461-28470.

Soardi, F. C., Barbaro, M., Lau, I. F., Lemos-Marini, S. H., Baptista, M. T., Guerra-Junior, G., . . . de Mello, M. P. (2008). Inhibition of CYP21A2 enzyme activity caused by novel missense mutations identified in Brazilian and Scandinavian patients. *J Clin Endocrinol Metab, 93*(6), 2416-2420. doi:10.1210/jc.2007-2594

Sorrenson, B., Suetani, R. J., Williams, M. J., Bickley, V. M., George, P. M., Jones, G. T., & McCormick, S. P. (2013). Functional rescue of mutant ABCA1 proteins by sodium 4-phenylbutyrate. *J Lipid Res, 54*(1), 55-62. doi:10.1194/jlr.M027193

Speiser, P. W., New, M. I., & White, P. C. (1988). Molecular genetic analysis of nonclassic steroid 21-hydroxylase deficiency associated with HLA-B14,DR1. *N Engl J Med, 319*(1), 19-23. doi:10.1056/NEJM198807073190104

Stikkelbroeck, N. M., Hoefsloot, L. H., de Wijs, I. J., Otten, B. J., Hermus, A. R., & Sistermans, E. A. (2003). CYP21 gene mutation analysis in 198 patients with 21-hydroxylase deficiency in The Netherlands: six novel mutations and a specific cluster of four mutations. *J Clin Endocrinol Metab, 88*(8), 3852-3859. doi:10.1210/jc.2002-021681

Stocco, D. M., & Clark, B. J. (1996). Regulation of the acute production of steroids in steroidogenic cells.

Endocr Rev, 17(3), 221-244. doi:10.1210/edrv-17-3-221

Tardy, V., Menassa, R., Sulmont, V., Lienhardt-Roussie, A., Lecointre, C., Brauner, R., . . . Morel, Y. (2010). Phenotype-genotype correlations of 13 rare CYP21A2 mutations detected in 46 patients affected with 21-hydroxylase deficiency and in one carrier. *J Clin Endocrinol Metab, 95*(3), 1288-1300. doi:10.1210/jc.2009-1202

Teter, S. A., Houry, W. A., Ang, D., Tradler, T., Rockabrand, D., Fischer, G., . . . Hartl, F. U. (1999). Polypeptide flux through bacterial Hsp70: DnaK cooperates with trigger factor in chaperoning nascent chains. *Cell, 97*(6), 755-765.

Tusie-Luna, M. T., Speiser, P. W., Dumic, M., New, M. I., & White, P. C. (1991). A mutation (Pro-30 to Leu) in CYP21 represents a potential nonclassic steroid 21-hydroxylase deficiency allele. *Mol Endocrinol, 5*(5), 685-692. doi:10.1210/mend-5-5-685

Tusie-Luna, M. T., Traktman, P., & White, P. C. (1990). Determination of functional effects of mutations in the steroid 21-hydroxylase gene (CYP21) using recombinant vaccinia virus. *J Biol Chem, 265*(34), 20916-20922.

Ulloa-Aguirre, A., Janovick, J. A., Brothers, S. P., & Conn, P. M. (2004). Pharmacologic rescue of conformationally-defective proteins: implications for the treatment of human disease. *Traffic, 5*(11), 821-837. doi:10.1111/j.1600-0854.2004.00232.x

Wedell, A. (2011). Molecular genetics of 21-hydroxylase deficiency. *Endocr Dev, 20*, 80-87. doi:10.1159/000321223

Wedell, A., Thilén, A., Ritzén, E. M., Stengler, B., & Luthman, H. (1994). Mutational spectrum of the steroid 21-hydroxylase gene in Sweden: implications for genetic diagnosis and association with disease manifestation. *J Clin Endocrinol Metab, 78*(5), 1145-1152. doi:10.1210/jcem.78.5.8175971

White, P. C., Grossberger, D., Onufer, B. J., Chaplin, D. D., New, M. I., Dupont, B., & Strominger, J. L. (1985). Two genes encoding steroid 21-hydroxylase are located near the genes encoding the fourth component of complement in man. *Proc Natl Acad Sci U S A, 82*(4), 1089-1093.

White, P. C., New, M. I., & Dupont, B. (1986). Structure of human steroid 21-hydroxylase genes. *Proc Natl Acad Sci U S A, 83*(14), 5111-5115.

White, P. C., & Speiser, P. W. (2000). Congenital adrenal hyperplasia due to 21-hydroxylase deficiency. *Endocr Rev, 21*(3), 245-291. doi:10.1210/edrv.21.3.0398

Xu, Z., Chen, W., Merke, D. P., & McDonnell, N. B. (2013). Comprehensive mutation analysis of the CYP21A2 gene: an efficient multistep approach to the molecular diagnosis of congenital adrenal hyperplasia. *J Mol Diagn, 15*(6), 745-753. doi:10.1016/j.jmoldx.2013.06.001

Xu, Z., Devlin, K. I., Ford, M. G., Nix, J. C., Qin, J., & Misra, S. (2006). Structure and interactions of the helical and U-box domains of CHIP, the C terminus of HSP70 interacting protein. *Biochemistry, 45*(15), 4749-4759. doi:10.1021/bi0601508

Yaffe, S. J., & Aranda, J. V. (2010). *Neonatal and pediatric pharmacology: therapeutic principles in practice*: Lippincott Williams & Wilkins.

Zeitlin, P. L., Diener-West, M., Rubenstein, R. C., Boyle, M. P., Lee, C. K., & Brass-Ernst, L. (2002). Evidence of CFTR function in cystic fibrosis after systemic administration of 4-phenylbutyrate. *Mol Ther, 6*(1), 119-126. doi:10.1006/mthe.2002.0639

Zhang, Y., Nijbroek, G., Sullivan, M. L., McCracken, A. A., Watkins, S. C., Michaelis, S., & Brodsky, J. L. (2001). Hsp70 molecular chaperone facilitates endoplasmic reticulum-associated protein degradation of cystic fibrosis transmembrane conductance regulator in yeast. *Mol Biol Cell,*

12(5), 1303-1314.

Zhao, B., Lei, L., Kagawa, N., Sundaramoorthy, M., Banerjee, S., Nagy, L. D., . . . Waterman, M. R. (2012). Three-dimensional structure of steroid 21-hydroxylase (cytochrome P450 21A2) with two substrates reveals locations of disease-associated variants. *J Biol Chem, 287*(13), 10613-10622. doi:10.1074/jbc.M111.323501

Zietkiewicz, S., Lewandowska, A., Stocki, P., & Liberek, K. (2006). Hsp70 chaperone machine remodels protein aggregates at the initial step of Hsp70-Hsp100-dependent disaggregation. *J Biol Chem, 281*(11), 7022-7029. doi:10.1074/jbc.M507893200

8. Appendix

Table 3 All data of density from western blots of reduced temperature and 4-PBA on WT and variant proteins

Protein (WT and variants)	*Time (min)*	*0*	*0.5*	*1*	*2*	*5*	*10*	*30*	*60*	*120*
WT 37°C	*1st*	4957632	3207204	1953612	2391084	3035772	1672920	770400	171936	260460
	2nd	4102138	4292366	4742362	4450218	3233534	2935234	1940052	2015406	3251926
	3rd	3711688	4427988	3898230	4937948	2767464	3996384	685216	768094	362862
	AVG	4257153	3975853	3531401	3926417	3012257	2868179	1131889	985145	1291749
	SEM	367929	386313	825672	780471	135056	671564	404829	543117	980534
WT 30°C	*1st*	5302044	3702744	3305736	3275676	2803844	2319996	1302984	820656	199188
	2nd	4135934	4026969	3172787	3057384	2569613	2182445	1238575	907943	235801
	3rd	4965972	4327690	3045754	5213186	2042312	2147746	854896	618936	117810
	AVG	4801317	4019134	3174759	3848749	2471923	2216729	1132152	782512	184266
	SEM	346548	180449	75057	685123	225196	52596	139869	85581	34869
WT 4PBA treated	*1st*	3331746	2939079	1509849	1553805	1380027	1502457	212784	37323	16764
	2nd	4502470	3772615	2418150	3074820	2116485	1828085	348390	340021	126420
	3rd	5027580	3123614	3102942	3700152	2206328	2007802	366792	11458	17884
	AVG	4287265	3278436	2343647	2776259	1900947	1779448	309322	129601	53689
	SEM	501231	252767	461393	637327	261748	147894	48560	105475	36367
P30L 37°C	*1st*	5601097	5850699	3066893	2280236	1450215	1262107	1054833	301920	81696
	2nd	8399330	5743586	5133040	4016334	3528300	1788052	2510850	1196848	1490246
	3rd	6887402	4160687	4506526	4759199	2747324	2647239	2314091	2222590	2675507
	4th	3276315	1958040	2047535	1582875	1512140	1408365	806260	642775	397060
	5th	5739812	5121794	4256358	3451612	3314932	3880352	2481728	2458234	2040374
	AVG	6656910	5219192	4240704	3626845	2760193	2394438	2090376	1544898	1571956

Protein (WT and variants)	***Time (min)***	***0***	***0.5***	***1***	***2***	***5***	***10***	***30***	***60***	***120***
	SEM	648393	387697	432532	522653	466720	571673	347893	496620	552629
P30Q 37°C	*1st*	5512519	2320196	3270023	2541382	1486253	1811927	1393087	746697	338735
	2nd	1567468	2339302	1877378	1658044	1642472	1040604	317254	111792	26860
	3rd	4524414	5259800	3785050	3057586	3757918	1968600	1123326	1893188	1059066
	AVG	5018467	3306433	2977484	2419004	1564363	1607044	944556	917226	474887
	SEM	1972526	976699	569792	408620	78110	286808	323173	521265	305650
P30L 30°C	*1st*	4102138	4292366	4742362	4450218	3233534	2935234	1940052	2015406	3251926
	2nd	6377105	6511435	5355525	6332585	3157175	3206560	1837080	1660225	989205
	3rd	6814844	5682406	7036270	4993088	3998498	2543264	1314116	1586196	737124
	AVG	5764696	5495402	5711386	5258630	3463069	2895019	1697083	1753942	1659418
	SEM	840828	647378	685682	559378	268620	192530	193777	132467	799572
P30Q 30°C	*1st*	1751832	1290744	1303236	872064	1179720	733320	1353852	415656	157968
	2nd	1567468	2339302	1877378	1658044	1642472	1040604	317254	111792	26860
	3rd	2134049	1149442	1316719	1319124	1219742	1211935	434380	556369	375291
	AVG	1942941	1815023	1499111	1283077	1347311	995286	375817	361272	186706
	SEM	191109	524279	189174	227608	148032	140010	58563	131187	101605
P30L 4PBA treated	*1st*	4102138	4292366	4742362	4450218	3233534	2935234	1940052	2015406	3251926
	2nd	6377105	6511435	5355525	6332585	3157175	3206560	1837080	1660225	989205
	3rd	6814844	5682406	7036270	4993088	3998498	2543264	1314116	1586196	737124
	AVG	5764696	5495402	5711386	5258630	3463069	2895019	1697083	1753942	1659418
	SEM	1010279	761902	634195	322200	289135	390067	356366	878836	1376534
P30Q 4PBA treated	*1st*	1751832	1290744	1303236	872064	1179720	733320	1353852	415656	157968
	2nd	1567468	2339302	1877378	1658044	1642472	1040604	317254	111792	26860
	3rd	2134049	1149442	1316719	1319124	1219742	1211935	434380	556369	375291
	AVG	1942941	1815023	1499111	1283077	1347311	995286	375817	361272	186706

Protein (WT and variants)	*Time (min)*	*0*	*0.5*	*1*	*2*	*5*	*10*	*30*	*60*	*120*
	SEM	357448	1422953	299440	781958	659440	948814	271699	217913	473796
G90V 37°C	*1st*	7151616	3333678	3459296	2871392	2051840	1426656	459744	57312	19968
	2nd	4360125	1602579	2455101	1553112	1134408	632412	126489	28545	19635
	3rd	2997088	2290176	748256	1011424	499680	1107424	470944	424000	350560
	4th	2589928	2527470	1296108	1696563	2119491	986733	701646	293667	761739
	AVG	4274689	2438476	1989690	1783123	1451355	1038306	439706	200881	287976
	SEM	1030966	357074	605431	391604	388708	164064	118355	95177	176116
G90V 30°C	*1st*	1224704	1320544	1851776	1078400	747008	506752	242752	9184	18496
	2nd	2072140	1897840	1853478	1333840	1119780	847230	200760	52395	148610
	3rd	2091111	1218492	1379103	1880676	836121	842919	405867	373923	204699
	4th	2390916	2724348	1290003	1669074	1451274	1315908	542223	463386	110451
	5th	2556736	1660640	2143104	1842560	1207776	778560	206656	235264	218624
	AVG	2067121	1764373	1703493	1560910	1072392	858274	319652	226830	140176
	SEM	229656	268803	160303	154540	127637	130328	67003	88166	36110
G90V 4PBA treated	*1st*	4926510	4010482	3421292	5445400	3055162	2426832	1863444	924350	1720108
	2nd	5720208	7106463	7220772	6299631	3387657	4341363	2349906	3361137	1811121
	3rd	4880016	3351888	1852776	2511396	2966508	2309040	2034000	1735092	434664
	AVG	5175578	4822944	4164947	4752142	3136442	3025745	2082450	2006860	1321964
	SEM	272646	1157480	1593593	1147190	128188	658687	142504	716444	444427
I172N 37°C	*1st*	5704560	6235092	3787452	3214260	3838068	2205720	2438424	3136932	1432296
	2nd	5801565	6499745	3906280	3388700	2141685	2789395	2987005	2022930	1946483
	3rd	7084152	7804044	7275564	4303872	4963068	3546180	3655728	3317004	3007872
	AVG	6196759	6846294	4989765	3635611	3647607	2847098	3027052	2825622	2128884
	SEM	444579	484931	1143414	337904	820012	388032	351975	404698	463883
I172N 30°C	*1st*	7133526	4830535	3024084	3697225	1323675	925592	1440484	1456949	38295

Protein (WT and variants)	*Time (min)*	*0*	*0.5*	*1*	*2*	*5*	*10*	*30*	*60*	*120*
	2nd	6814198	4549208	4459680	3740986	2806528	2661824	2317316	1821720	561792
	3rd	7874562	7152100	4058381	3633521	3531587	2576902	1906758	692233	71336
	AVG	7274095	5510614	3847382	3690577	2553930	2054773	1888186	1323634	223808
	SEM	314066	824751	427639	31200	649762	565122	253290	332799	169261
I172N 4PBA treated	*1st*	11916110	8037658	8878335	5002992	5194245	4905201	4599544	2258295	2346318
	2nd	10098580	6705504	5653332	6909912	13061300	4281056	3383384	2390460	2359680
	3rd	13174100	10262660	6969116	7613518	8581158	6212616	4905724	3524100	502962
	AVG	11729597	8335274	7166928	6508807	8945568	5132958	4296217	2724285	1736320
	SEM	892711	1037589	936217	779824	2278321	569103	464896	401723	616691
V281G 37°C	*1st*	1978496	2044160	1359392	1995424	301408	252544	161984	65184	57696
	2nd	1812030	1146985	1257060	801710	802865	643440	288995	312970	246925
	3rd	2411552	2173312	2035520	1737344	967680	1119200	728800	706432	356672
	AVG	2067359	1788152	1550657	1511493	690651	671728	393260	361529	220431
	SEM	178680	322744	244224	362627	200353	250582	171730	186698	87318
V281L 37°C	*1st*	4423774	2817172	2683688	6274020.	4448594.	1548666	212194	208556	145656
	2nd	2375345	1795808	1950048	3111392.	1310208	1202720	590208	380416	500960
	3rd	2985567	2577600	1928352	1886304	2140256.	1342720	850592	482752	431104
	4th	4957632	3207204	1953612.	2391084	3035772	1672920	770400	171936	260460
	5th	4102138	4292366	4742362	4450218	3233534	2935234	1940052	2015406	3251926.*
	6th	3711688	4427988	3898230	4937948	2767464	3996384	685216	768094	362862
	AVG	3759357	3186356	3040536	2909202	2586745	1441757	841444	671193	340208
	SEM	387785	416567	556116	784166	436097	104807	237736	282822	62780
V281G 30°C	*1st*	3915795	4356846	3380949	2106195	2430246	1710540	1676142	888693	1030653
	2nd	4028893	2400116	2115179	2601988	1253930	803048	351093	237355	42624
	3rd	5382470	4196552	4212144	3196338	3125954	2434200	2578866	2066588	743104

Protein (WT and variants)	*Time (min)*	*0*	*0.5*	*1*	*2*	*5*	*10*	*30*	*60*	*120*
	AVG	4442386	3651171	3236091	2634840	2270043	1649263	1535367	1064212	605460
	SEM	471175	627237	609659	315126	546311	471869	646943	535297	293405
V281L 30°C	*1st*	1658283	1338381	1019436	1101177	861663	577632	321915	267762	101574
	2nd	1654950	1685754	1373158	959208	929968	689146	409802	148988	104992
	3rd	2367024	1941885	1655676	2007390	1029270	861531	688215	299310	279807
	4th	5302044	3702744	3305736	3275676	2603844	2019996	1302984	820656	199188
	AVG	2745575	2167191	1838502	1835863	1356186	1037076	680729	384179	171390
	SEM	868452	526576	506097	533133	417307	332803	221624	149048	42632
D322G 37°C	*1st*	5072935	6130390	4105780	3735725	3900190	2308180	5047735	1864660	1956710
	2nd	6523560	5741172	11481160	3951252	4952124	1496124	2982024	1921680	452340
	3rd	4076205	3546642	4650393	2502465	1483185	1153086	406560	241329	8349
	AVG	5224233	5139401	6745778	3396481	3445166	1652463	2812106	1342556	805800
	SEM	550374	804267	2372905	451317	1026916	342487	1342483	550860	589556
D322G 30°C	*1st*	3354540	3622150	2409120	3471755	1865080	2407545	1245090	1811565	519330
	2nd	10093030	7013356	5687422	6000124	5529608	5185138	3954318	2972854	3345634
	3rd	3122388	1977156	1883088	1807200	1353528	608580	754956	827352	361368
	AVG	5523319	4204221	3326543	3759693	2916072	2733754	1984788	1870590	1408777
	SEM	2285838	1482670	1190166	1218925	1315085	1331169	994878	620056	969501
R356Q 37°C	*1st*	11820890	6403572	5655312	5654448	4618332	3293424	2629872	1865700	594972
	2nd	5696600	4830735	2540125	2767380	2356165	1904035	1261540	1067045	1617140
	3rd	7261452	7448976	3789972	3853836	3847824	3681684	2045952	1758168	1669032
	AVG	8259647	6227761	3995136	4091888	3607440	2959714	1979121	1563638	1293715
	SEM	1837029	760916	905109	841881	664000	539608	396414	250229	349692
R356W 37°C	*1st*	6390825	3741500	3954545	1416905	5162255	1941975	1948905	1069495	1334270
	2nd	6706398	4851403	3618156	3273575	3108851	2810335	2849000	2016611	2203498

Protein (WT and variants)	*Time (min)*	*0*	*0.5*	*1*	*2*	*5*	*10*	*30*	*60*	*120*
	3rd	6135290	4627420	2877525	1645595	1270605	2239790	876435	1090565	1016785
	AVG	6410838	4406774	3483409	2112025	3180570	2330700	1891447	1392224	1518184
	SEM	165168	338863	318125	584515	1123995	254762	570155	312253	354702
R356Q 30°C	*1st*	1732230	2351934	1675458	1293672	1607134	408462	904210	312208	311828
	2nd	2170662	1903558	1215772	1380366	1116764	992120	1193264	705296	30974
	3rd	3883790	3934102	3340504	2309450	1995456	1984474	1495148	1244196	1093298
	AVG	2595561	2729865	2077245	1661163	1573118	1128352	1197541	753900	478700
	SEM	656431	615874	645419	325108	254226	460026	170603	270137	317814
R356W 30°C	*1st*	3179965	4323043	3154916	2869646	2918042	1995521	1443888	1068227	811447
	2nd	1153116	1284552	832104	735156	722484	727324	152216	64152	25128
	3rd	5851764	6894216	5703588	5325552	4050252	3692628	2737944	1843236	933876
	AVG	3394948	4167270	3230203	2976785	2563593	2138491	1444683	991872	590150
	SEM	1360635	1621242	1406780	1326216	976855	858989	746435	514994	284713
R356Q 4PBA treated	*1st*	8876016	10715580	6336252	9032220	9410795	3541932	2532600	1831356	290340
	2nd	8174232	13246740	14764250	10012680	8952480	4580784	6974820	4238568	1726308
	3rd	5166404	4766986	4452992	6131566	3300022	2466590	3773362	1294204	751640
	AVG	7405551	9576435	8517831	8392155	7221099	3529769	4426927	2454709	922763
	SEM	1137755	2513284	3170172	1165193	1964998	610346	1323341	905308	423266
R356W 4PBA treated	*1st*	6188256	5339664	2966292	5519412	4926060	4325940	1913364	2508480	1109376
	2nd	12228650	8822205	10997420	10450790	13266260	6823880	3464860	2399845	1637160
	3rd	5230320	10647600	4184034	7426986	6803118	2599472	1938319	782476	603914
	AVG	7882409	8269823	6049249	7799063	8331813	4583097	2438848	1896934	1116817
	SEM	2190645	1556962	2498935	1435671	2526026	1226241	513057	558111	298296
G375S 37°C	*1st*	3585420	6553188	3848976	3895416	2468700	1792512	1403424	1505304	1459368
	2nd	4730364	6422904	4547448	5086764	2278332	2806560	1983096	2895084	1193976

Protein (WT and variants)	*Time (min)*	*0*	*0.5*	*1*	*2*	*5*	*10*	*30*	*60*	*120*
	3rd	3210725	3854935	3739610	3807160	1985410	2579640	1809535	2359525	3289090
	AVG	3842170	5610342	4045345	4263113	2244147	2392904	1732018	2253304	1980811
	SEM	457080	878509	253029	412613	140557	307260	171767	404695	658610
G375S 30°C	*1st*	3965472	6257556	2170224	3211812	2244780	977760	866736	834012	201708
	2nd	2653980	2232685	2819950	1758855	1297870	955290	1214605	301805	177485
	3rd	6211523	4486509	5503306	4698371	2965735	5123168	2085061	1162688	1831019
	AVG	4276992	4325583	3497827	3223013	2169462	2352073	1388801	766168	736737
	SEM	1038719	1164663	1020130	848584	482942	1385563	362324	250820	547186
P453S 37°C	*1st*	7878852	5742144	4843296	4326264	4344336	3444588	1624572	1517940	1401840
	2nd	3888444	4434722	5849054	3420128	2815676	2083180	1020000	700230	502010
	3rd	5555838	4711516	4755682	4053072	3611956	3333326	2544934	2135370	2126326
	AVG	5774378	4962794	5149344	3933155	3590656	2953698	1729835	1451180	1343392
	SEM	1157103	397783	350768	268363	441415	436442	443346	415632	469809
P453S 30°C	*1st*	4686272	4263029	4179372	2767970	3160614	1796091	1766158	763606	563214
	2nd	3151512	2519663	3006583	3811703	2054499	1469788	959706	803418	316387
	3rd	7212286	6738578	6561460	4476856	4753002	4297306	2757774	2147874	1741198
	AVG	5016690	4507090	4582472	3685510	3322705	2521062	1827879	1238299	873600
	SEM	1183829	1223994	1045810	497332	783195	893103	519974	454933	439612
R483Q 37°C	*1st*	5373576	2601036	3861936	3604788	2076300	3765348	1480068	4140072	1202940
	2nd	3218296	5864008	4325654	3952342	2500742	2250208	2183252	856292	947226
	3rd	6700005	3464097	3873246	4749498	2540226	2173587	1705080	3173274	1109433
	AVG	5097292	3976380	4020279	4102209	2372423	2729714	1789467	2723213	1086533
	SEM	1014532	976144	152723	338839	148499	518289	207330	974289	74701
R483W 37°C	*1st*	3093524	1437249	1673001	1398771	1347126	993762	316899	683892	492987
	2nd	2886176	1815872	1516000	671872	738720	279392	205504	220256	104352

Protein (WT and variants)	*Time (min)*	*0*	*0.5*	*1*	*2*	*5*	*10*	*30*	*60*	*120*
	3rd	809550	477085	539210	405650	444080	232995	354690	345765	83370
	AVG	2263083	1243402	1242737	825431	843309	502050	292364	416638	226903
	SEM	729227	398443	354671	296793	265880	246221	44779	138452	133180
R483Q 30°C	*1st*	4159365	4216520	3433850	2742120	3896770	2069655	1594740	1333675	827295
	2nd	4643892	3487320	4096696	3091150	2077472	1620848	891648	1347516	915732
	3rd	2196324	2653008	2319786	1463266	1411358	1716384	1081860	660972	600400
	AVG	3666527	3452283	3283444	2432179	1744415	1802296	1189416	1114054	781142
	SEM	748290	451687	518433	494823	333057	136495	209969	226576	93908
R483W 30°C	*1st*	1118362	1037702	1120730	524438	277463	772634	294224	203648	13135
	2nd	330400	753340	892745	548450	291235	235760	346815	378000	124565
	3rd	9137408	7213600	6111168	3317600	1192864	2756224	920224	727584	43232
	AVG	3528723	3001547	2708214	1463496	587187	1254873	520421	436411	60311
	SEM	2813552	2107626	1702749	927078	302864	766507	200477	154041	33281
R483Q 4PBA treated	*1st*	7559388	5592708	5056308	3437964	5292000	4193352	2051724	1058256	893844
	2nd	5258884	2198762	2823581	4384426	3271392	2334441	2142226	3181371	589558
	3rd	7664090	5087705	6869765	4915435	5558665	4136440	3633315	2441845	2103745
	AVG	6827454	4293058	4916551	4245942	4707352	3554744	2609088	2227157	1195716
	SEM	784867	1057247	1170121	432093	722095	610373	512779	622220	462434
R483W 4PBA treated	*1st*	3525552	2054700	3482748	1487844	3628116	1095732	1451520	1058256	320868
	2nd	6017935	4027835	3493140	3856860	2787855	2695000	1325975	1756090	1358035
	3rd	4986648	3189024	2854872	2946492	2444364	1231200	1101168	1000332	443304
	AVG	4843378	3090520	3276920	2763732	2953445	1673977	1292888	1271559	707402
	SEM	723046	571720	211045	689954	351607	512007	102482	242842	327231

The densities of the Western blot bands were quantified with Image Lab™ software, expressed in arbitrary units (AU) after scanning optical density.

Table 4 Comparison of half-lives from variant protein pairs which have the same mutation site

P value	***P30L vs P30Q***	***V281G vs V281L***	***R356Q vs R356W***	***R483Q vs R483W***
37°C	0.008	<0.001	0.027	<0.001
30°C	0.020	<0.001	<0.001	<0.001
4PBA treated	0.008		<0.001	<0.001

9. Acknowledgments

At the end of thesis, I would like to thank all those who made this thesis possible.

First of all, I would like to express my deepest gratitude to my respectable supervisor PD Dr. Nicole Reisch, who offered her continuous supervision and encouragement throughout the whole thesis. She helped me to overcome every difficulty in the design and process of the experiments. Without her consistent and illuminating instruction, the thesis could not have reached its present form.

I would also like to express my thanks to the BTA Kerstin Schaefer, who is no doubt warm-hearted and helpful to my experiment. She helped me prepare materials of my experiment and taught me some techniques of the experiment, thus making the downstream experiment possible. And she as a friend also helps me solving life problems to make me get used to the environment in Munich.

Besides, many thanks to every colleague in the endocrinology department. They are always so friendly and enthusiastic. We spent together wonderful two years. I have been so fortunate to meet these people.

Last but not the least, I would like to thank my parents and my husband for supporting me spiritually throughout my life.